BRNO UNIVERSITY OF TECHNOLOGY
VYSOKÉ UČENÍ TECHNICKÉ V BRNĚ

FACULTY OF MECHANICAL ENGINEERING
FAKULTA STROJNÍHO INŽENÝRSTVÍ

INSTITUTE OF AUTOMOTIVE ENGINEERING
ÚSTAV AUTOMOBILNÍHO A DOPRAVNÍHO INŽENÝRSTVÍ

ELECTRIC CAR VERTICAL DOOR OPENING SYSTEM DESIGN
NÁVRH SYSTÉMU VERTIKÁLNÍHO OTEVÍRÁNÍ DVEŘÍ ELEKTROMOBILU

MASTER'S THESIS
DIPLOMOVÁ PRÁCE

AUTHOR — **Bc. Tomáš Kolečář**
AUTOR PRÁCE

SUPERVISOR — **Ing. Pavel Ramík**
VEDOUCÍ PRÁCE

BRNO 2018

VYSOKÉ UČENÍ TECHNICKÉ V BRNĚ
FAKULTA STROJNÍHO INŽENÝRSTVÍ

Zadání diplomové práce

Ústav:	Ústav automobilního a dopravního inženýrství
Student:	**Bc. Tomáš Kolečář**
Studijní program:	Strojní inženýrství
Studijní obor:	Automobilní a dopravní inženýrství
Vedoucí práce:	**Ing. Pavel Ramík**
Akademický rok:	2017/18

Ředitel ústavu Vám v souladu se zákonem č. 111/1998 o vysokých školách a se Studijním a zkušebním řádem VUT v Brně určuje následující téma diplomové práce:

Návrh systému vertikálního otevírání dveří elektromobilu

Stručná charakteristika problematiky úkolu:

Náplní práce je provedení konstrukčního návrhu systému vertikálního otevírání dveří elektromobilu pro převážně městský provoz.

Cíle diplomové práce:

Provést rešerši používaných systémů otevírání dveří osobních automobilů se zaměřením na vertikální otevírání.
Navrhnout koncepci vertikálního mechanismu pro otevírání předních dveří elektrického vozidla Uniti při zohlednění požadavků na něj kladených.
Navrhnout vhodný pohon mechanismu pro automatické otevírání dveří.
Provést konstrukční návrh dílů mechanismu otevírání dveří v CAD systému a provést s tím související počítačové simulace.
Začlenit navržený mechanismus do sestavy vozidla s možností parametrických úprav.
Zhodnotit navrženou konstrukci a vyslovit se k vhodnosti jejího použití pro uvažovaný elektromobil.

Seznam doporučené literatury:

MORELLO, Lorenzo, et. al. The Automotive Body. Dordrecht: Springer Verlag, 2011. 668 s. ISBN 978-94-007-0512-8.

BUDYNAS, Richard G., NISBETT, J. Keith a SHIGLEY, Joseph Edward. Shigley's mechanical engineering design. 10th edition. New York, NY: McGraw-Hill Education, 2015. 1104 s. ISBN 0073398209.

KLEIN, Bernd. FEM Grundlagen und Anwendungen der Finite-Element-Methode im Maschinen- und Fahrzeugbau. Wiesbaden: Vieweg + Teubner Verlag, 2012. 428 s. ISBN 978-3-8348-1603-0.

Termín odevzdání diplomové práce je stanoven časovým plánem akademického roku 2017/18.

V Brně, dne 27. 10. 2017

VYSOKÉ UČENÍ TECHNICKÉ V BRNĚ FAKULTA STROJNÍHO INŽENÝRSTVÍ DĚKANÁT

L. S.

prof. Ing. Václav Píštěk, DrSc.
ředitel ústavu

doc. Ing. Jaroslav Katolický, Ph.D.
děkan fakulty

ABSTRAKT

Cílem této diplomové práce je výběr vhodného mechanismu automatického otevírání dveří pro elektromobil kategorie EU L7e. Pomocí analýzy dostupných řešení na trhu jsou k bližšímu zkoumání zvoleny tři koncepty. Klíčové prvky nejvhodnějšího mechanismu jsou navrženy s ohledem na silové působení včetně volby vhodného typu aktuátoru. V závěru práce je sestava zhodnocena s ohledem na předem zadané uživatelské požadavky.

KLÍČOVÁ SLOVA

Vertikální otevírání dveří, elektromobil, Uniti

ABSTRACT

The main aim of this diploma thesis is to select the most appropriate automatic door mechanism for an electric vehicle of category EU L7e. With the aid of the market analysis three concepts were selected for detail observation. Crucial parts of the most appropriate system assembly were designed with respect to load conditions. At the end of the thesis there is an assessment of the proposed assembly according to user requirements.

KEYWORDS

Vertical opening door mechanism, electric vehicle, Uniti

BIBLIOGRAFIC CITATION

KOLEČÁŘ, T. Eletric car vertical door opening system design. Brno: Brno University of Technology, Faculty of Mechanical Engineering, 2018. 101 pages. Supervised by Ing. Pavel Ramík.

DECLARATION OF ORIGINALITY

I hereby declare that the master's thesis on the topic Electric Car Vertical Door Opening System Design I wrote independly under guidance of the master's thesis supervisor and using literature and other sources of information which are all quoted in the thesis and detailed in the list of literature at the end of the thesis.

Brno 28. October 2017 ……..……..……..

Tomáš Kolečář

ACKNOWLEDGEMENT

I would like to express gratitude to my supervisor Ing. Pavel Ramík for useful recommendations and help during my whole studies at Brno University of Technology.

I am very grateful to my parents, who have always supported me my whole life.

CONTENTS

INTRODUCTION

The revolution in the automotive industry is happening now and it is inevitable. Trends in the production and development of transport equipment in recent decades have been changing as a result of the drive to use electric vehicles and the application of autonomous systems. The incentive to transform electricity-using transport instead of using fossil fuels is primarily to reduce exhaust and noise emissions. Autonomous systems applied to transport vehicles aim to increase road safety and increase traffic efficiency.

The solved problem of this diploma thesis is the design of the automatic mechanism of opening the door applied on a two-seat electric car Uniti. Product Uniti is a lightweight electric city car that must meet the regulations of heavy quadricycles (EU L7e). The vehicle includes Steer-by-Wire system, driver assist features and a full-screen Head-up Display industry. The development process of the car started in summer 2016. First deliveries of vehicles to market are planed for in 2020. General technical specification [1]:

- maximal speed of 90km/h,
- 15kW AC motor,
- 400kg weight,
- 11kWh Na-Ion battery,
- Induction or plug-in charge,
- 150kg range,
- designed for autonomy,
- predominantly made of biomaterials,
- driver interface based on human biomechanics.

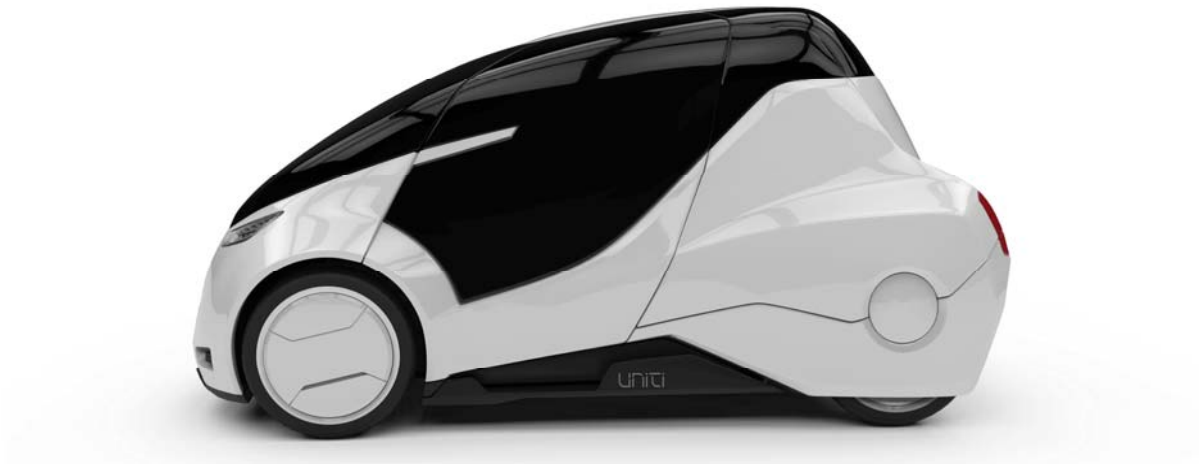

Fig. 1.1: Electric vehicle Uniti [1]

The first part of this work introduces to the reader the most distinctive vertical door opening mechanisms of the vehicles that have been introduced to the market. The following chapter describes the requirements for the specified system. The chapter safety analysis deals with possible hazard situations that may occur during the use of the vehicle. Then, selected concepts are created by using CAD (Computer-Aided-Design) systems and incorporated into a simplified assembly of the vehicle. In the next chapter, the most appropriate variant is selected, which is subjected to kinematic and dynamic analysis. On the basis of the obtained calculations and simulations, a more detailed design is made including suitable types selection of the most important components. Because of the initial stage of the development, the position of the surrounding parts is not fixed, so attention is paid only to the core elements of the assembly. The final part of the work is devoted to the evaluation of the design including recommended methods for verification of the structure in its further development and with regard to the use of safety elements. This thesis does not deal with the software part of the actuator control.

Fig. 1.2: Vehicle Uniti with opened doors [2]

1 SCISSOR DOORS

Scissor doors are automobile doors that rotate vertically at a fixed hinge, rather outward as with conventional door. The first vehicle to feature scissor door was the 1968 Alfa Romeo Cabaro concept car by Bertone's Marcello Gandini. The first production car to feature the scissor doors was Lamborghini. The Aventador is the latest car to feature the trademark scissor doors which are ussually called as „Lambo style doors“. Today many aftermarket companies are specialized in production of scissor door conversation kits for regular production cars.

Advantages:

- offer the possibility of operating the vehicle with the door open,
- thinner parking space is allowed (doors are opened upwards),
- reduces the dooring hazard for pedestrians and cyclists,
- convertible version of the car is possible with the same door style.

Disadvantages:

- higher manufacturing costs,
- limited height of a parking lot,
- vehicle egress may be impossible in a rollover accident.

The most automotive corporations are focused on constant development of their products. This is related to design studies which often represent modern ideas and shape other vehicles. In this conceptual phase, designers have a lot of space for innovation. Their aim is the introduction of new unique systems that attract customers. Even if new technical innovations do not immediately find use, they are patented. There are dozens of patented door systems that have not been used in series. Owners of these patents are mostly companies focusing on sports or premium quality vehicles.

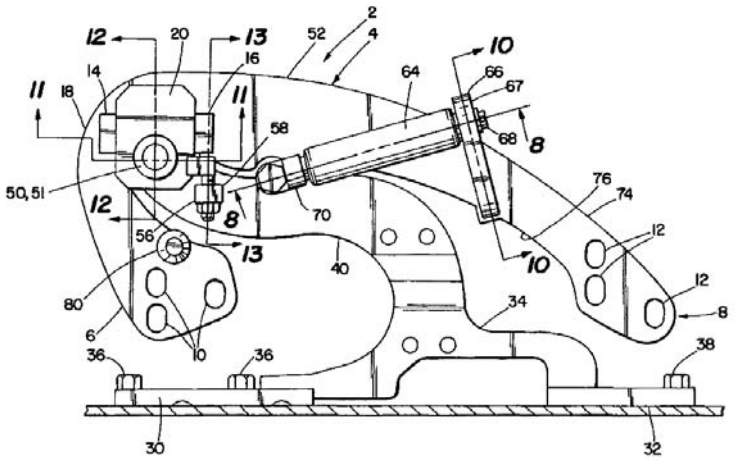

Fig.1.1: Lamborgini patent [3]

1.1 LAMBORGINI AVENTADOR

Pioneer in the area of using sccisor door is Italian company Lamborgini. The Lamborghini Aventador is a mid-engined sports car produced by an Italian manufacture. It was launched on 28 February 2011 at Geneva Motor Show. The doors opening system is based on mechanical hinges. There exist also aftermarket kits which allow customers door opening or closing by a remote control. These kits require electric or hydraulic actuator. After the opening process the door remain in 60 degrees from the horizontal plane.

Fig. 1.2: Lamborgini Aventador [4]

1.2 KOENIGSEGG AGERA

Swedish company Koenigsegg is focused on development and production of luxury sport cars. In model Agera there is used the system visualised in figure 1.3. This solution contains the arm attached to the pivot. During a motion of the door to the side gearing revolves with door in upper direction around 90 deg. In the end position the door is almost upright. In model Agera there is implemented a hydraulic unit which is connected to the hydraulic system. A user can open or close the door automatically by the hydraulic actuator. The Koenigsegg design is unique and also patented.

Fig. 1.3: Koenigsegg Agera door mechanism system [5][6]

1.3 ALFA ROMEO PANDION

The prototype of Alfa Romeo - Pandion was introduced at International Show in Geneva 2010. This car impressed visitors by the unusual opening of the door. When opening and closing the door, not only the door, but also the part of the bodywork in the front and rear of the vehicle, is moving. As with the Aventador, the mechanism is automatically controlled by the actuator. A disadvantage of this system is high demands on the actuator in terms of forces acting (large moments of inertia) and the cost of the door guidance system. The Alfa Romeo system has not been used in production yet.

Virtually hinged around the axis of the rear wheel, the Pandion doors open by rotating backwards, ending up a perfect 90 degrees above the center of the rear wheel, lifting up the entire body side of the vehicle, from the front fender to the rear fender. When fully open they are more than 3.6 metres high. This spectacular solution is design mainly for glamour. This futuristic door mechanism also has a pragmatic side as well. Since all 'extreme' sports cars are literally impossible to get in and out of, the Pandion is designed to utilize the horizontal space in the car since the vertical space is so limited. [7]

Fig. 1.4: Alfa Romeo Pandion prototype at International show in Geneva 2010 [8]

1.4 TATA PIXEL

In Asia, the number of vehicle manufacturers of all kinds is rapidaly growing. An Indian company introduced the model of mass-produced electric vehicle Angkor. The vehicle door rotates around a single axis. In this case, an electric actuator is used. The door allow egress to both front and rear seat passenger crew.

Fig. 1.5: Tata Pixel [9]

1.5 TOYOTA CONCEPT-I

In January 2017 Toyota has introduced the Concept-I at CES (a global consumer electronics and consumer technology tradeshow in Las Vegas). Toyota´s concept is based on elegant futuristic designed interior and exterior accompanied by the latest electronic systems. This vehicle is powered by electric motors and utilizes many interactive elements.

From the perspective of door mechanism, Toyota has equipped Concept-I by automatic system. Door movement is divided to separate translation and rotational motion. After the door extrusion, the door structure is revolved around the front axle of the axis of the wheel. The mechanism is shown in the figure below.

Fig. 1.6: Toyota Concept-i [10]

2 SYSTEM DEVELOPMENT PROCESS

There exist several ways of the product development. In this chapter are described two wildly used design processes. Based on their comparison will be selected more suitable method for further door system development.

2.1 WATERFALL MODEL

The waterfall development model is sequential design process. In a waterfall model, each phase must be completed fully before the next phase can begin. Its progress is seen as flowing steadily downwards (like a waterfall) through the phases of conception, initiation, analysis, design, construction, testing, production/implementation and maintenance. [11]

This development model originates in the manufacturing and construction industries: highly structured physical environments in which after-the-fact changes are prohibitively costly, if not impossible. Nowadays this process is widly used also in software development departments.

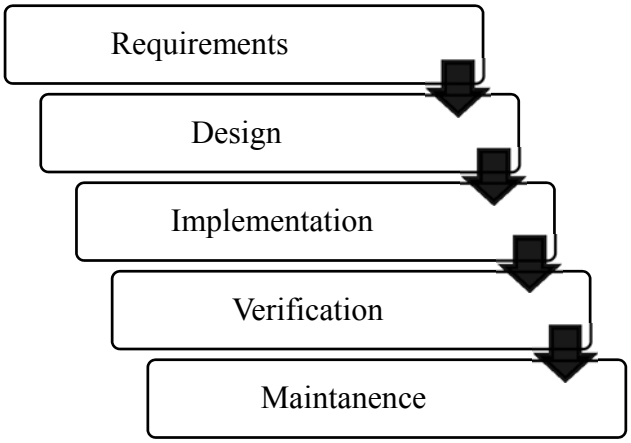

Fig. 2.1: The waterfall diagram

Advantages:

- simple and easy to understand model,
- easy to manage due to rigidity of the model,
- works well for smaller projects where requirements are very well understood.

Disadvantages:

- once an application is in the testing stage, it is difficult to change the concept idea,
- high degree of risk and uncertainty,
- not a good tool for large or complex projects,
- a poor model for a long going projects. [11]

2.2 V-MODEL

In the past decade V model became the most used method not only in automotive industry. In figure 2.2 there is shown the layout of its structure. The development process is divided into two main sections depending on each other (design and verification) which include a particular sub steps. The biggest advantage of this system is prevention to make a wrong decision due to interconnection of each parts.

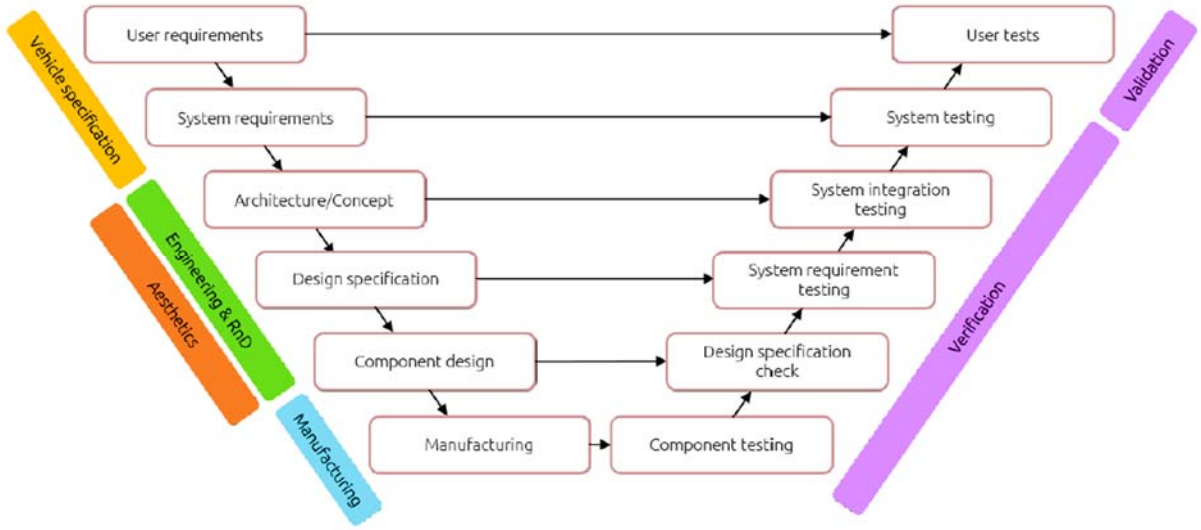

Fig. 2.2: Schema of V-model [12]

Advantages:

- simple and easy to use
- system defects and failures can be found at early stage
- works well for small but also for medium sized projects

Disadvantages:

- very rigid and the least flexible,
- if any changes happen in midway, then the documents along with requirements have to be updated. [11]

Within the scope of this thesis is to proceed through phases analogous to V model. In this thesis most of the attention is paid to system specification, user requirements, concept description, engineering design and safety analysis. Manufacturing, verification and validation processes are mentioned as suggestions for onward development.

3 DOOR MECHANISM DESIGN

Development of door mechanism must consider a lot of aspects with regard to user requirements. Since this is a completely new vehicle development, there is quite a lot of space for innovation and technical solutions. However, the proposal must be safe for the user at all times.

3.1 USER REQUIREMENTS

To create a design proposal, it is necessary to take into account all the demands placed on the system. These requirements specify the expected function and define the boundary conditions that need to be respected in the next process. It is appropriate at the beginning of the development process to specify and quantify the requirements that the product should meet. According to the V-Model, at the end of the development cycle, it must match the properties of the final product.

3.1.1 General requirements

General user requirements can be divided into groups including consideration of security functionality, aesthetics and cost. Specific requirements for vertical opening door include:

Safety:

- consider all operating situations,
- prevent collision during door opening,
- prevent injury of passengers during door opening/ closing.

Functionality:

- operated automatically with the possibility to open manually,
- reliability 150 000km,
- smooth variable movement – non-linear opening and closing,
- opening speed between 3 up to 5 seconds,
- quiet actuator,
- rigid construction, avoid vibration during movement,
- all parts (struts, actuators) must work during different weather conditions (-30; 50)°C.

It is obvious that some of the points are ambiguous and need a more detailed specification. Therefore, they are further specified. Consideration of "all possible situations" means that the door is safe not only for normal traffic but also for a vehicle accident situation.

3.1.2 System reability

Reliability of the entire car has to meet at least 150 000km of road traffic. In order to estimate the lifetime of the door opening mechanism components must be considered. A simplified *"HWSSH"* model has been created to represent the average Uniti user´s behaviour in the age range between 25 to 60 years old. Because the vehicle is designed for city traffic, the average distance of 30 km per day is expected. During this trajectory, the user performs a route from home to work, to school, to a shop and ends his journey at home. During each stop there will be one opening and one closing of the door. That means 10 opening / closing per day. From the reability perspective, the mechanism should withstand at least 50 000 cycles.

3.1.3 SYSTEM MOTION

The primary movement of the door is a rotation around the front wheel axle. Secondary movement is the translational movement of the door to the side which prevents the collision of the door with the bodywork. From the viewpoint of possible collisions with the surrounding environment, the door must not be in contact with a 20 cm barrier (representing a curb). Based on the market analysis, opening times of available door mechanisms have been identified. These times represent the average of 5 values measured while watching available videos.

Tab. 3.1: Comparation of opening times

Vehicle	Actuator type	Opening time [s]
Koenigsegg Agera	hydraulic	3,0
Tata Pixel	electric	6,1
Angkor	eletric	6,5
Alfa Romeo Pandion	eletric	15,2
Toyota Concept i	electric	7,1

Based on consultation with the technical department it was decided to set the time interval for opening the door electric vehicle Uniti 5 seconds. A lower opening time would cause a higher dynamic load on the system. Another requirement was nonlinear smooth movement of the door.

Fig. 3.1: External environment boundaries represents a curb (red)

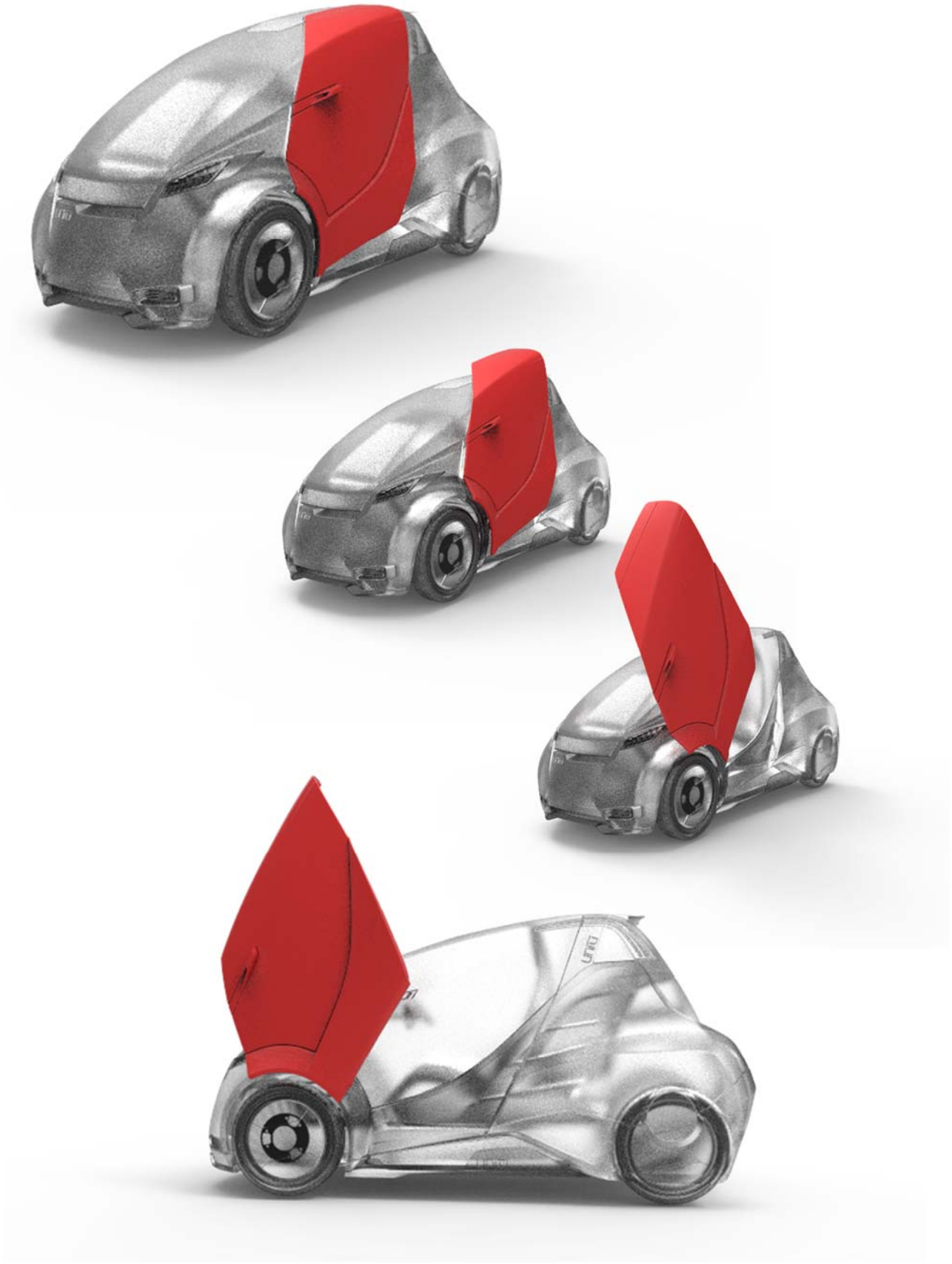

Fig. 3.2: Ideal proposal of door motion at 0s, 2s and 5s

3.2 SYSTEM REQUIREMENTS

In the system of the automatic door mechanism there are four main subsystems: chassis, door, door mechanism and electronics. The situation is described on the diagram of the system:

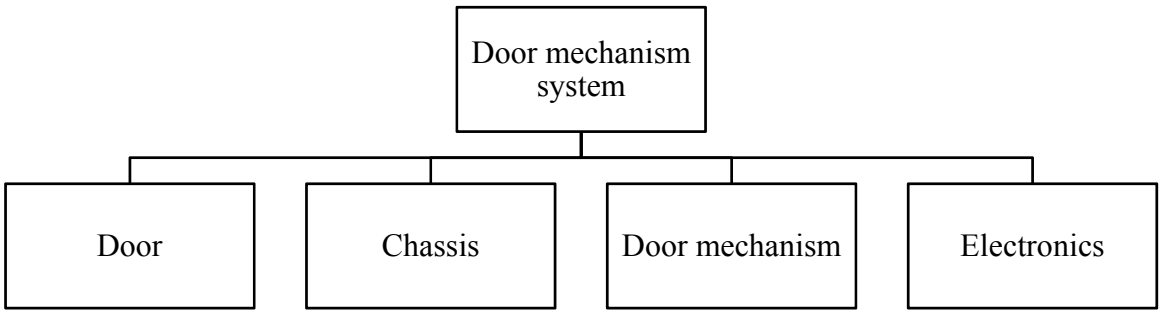

Fig. 3.3: Door mechanism system diagram

In terms of design it was necessary to get parameters of the system to define the boundary conditions. By using these parameters, it is possible to continue in the system design with respect to other parts of the vehicle.

3.2.1 DOOR

The technical section was provided by the CAD model in * .obj format. To obtain paramters such as weight, position of the center of gravity of the door, including its moments of inertia, a new solid model was needed. The PTC Creo Parametric 3.0 software was used to create the model.

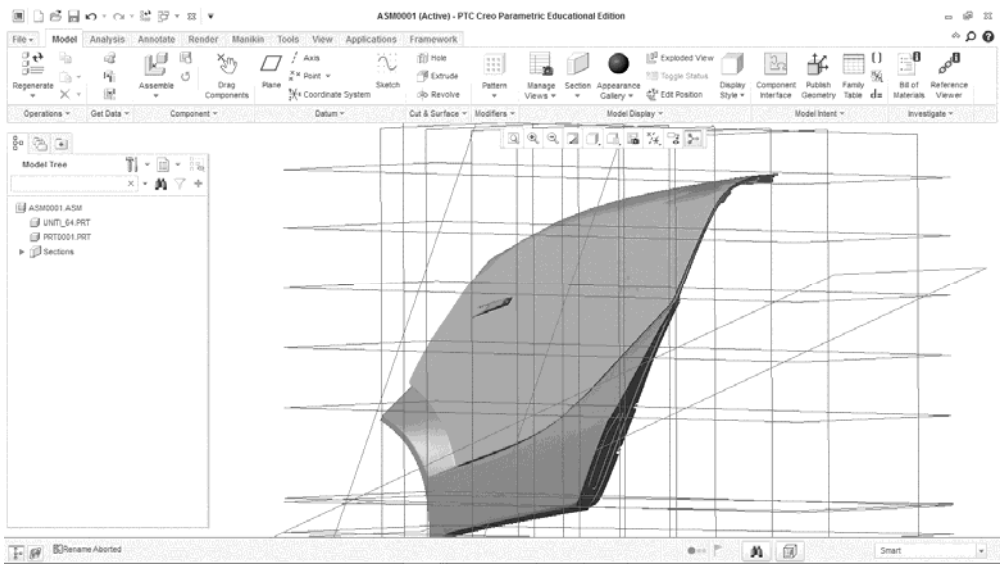

Fig. 3.4: Reverse engineering in software PTC Creo Parametric 3.0

Material properties were assigned after creating the solid model. The transparent part of the door is considered as polycarbonate. Door structure has composite structure properties. Material densities are listed in the table below:

Tab. 3.2: Density of considered materials [13]

Material	Density [kg/m^3]
Polycarbonate	1200
CFRP Laminate (graphite)	1500

Although this is the initial model, not including all door elements and details, it provides valuable information about the position of the center of gravity and moment of inertia. These parameters are essential for futher assembly design. Part of this work is also modification of the door shape for a suitable implementation of the new system. Principal moment of inertia parallel to the door rotation axix is 4,72kg.m^2. Total door weight is 16,03kg.

Tab. 3.3: Weight distribution of side door measured in CAD

Section name	Weight [kg]
5 mm thin polycarbonate side structure	7,71
composite structure	8,32

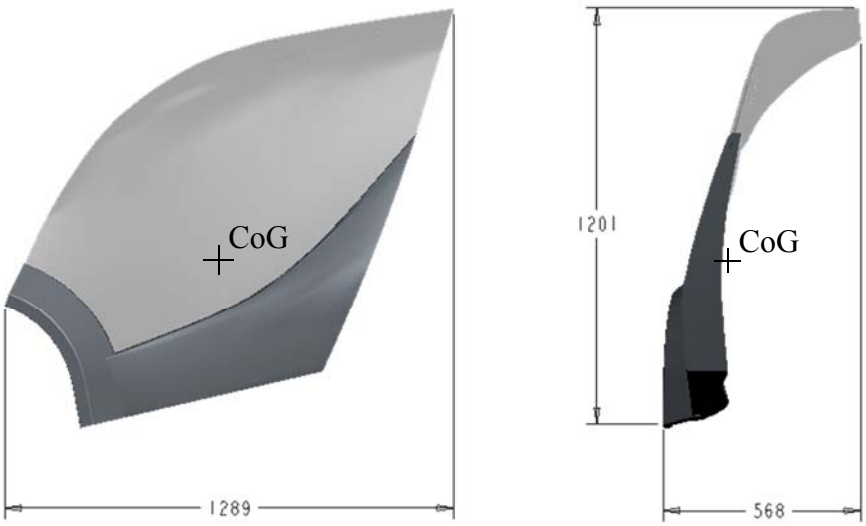

Fig. 3.5: View on 3D CAD solid model with highlighted general dimensions [mm]

3.2.2 CHASSIS

Another significant system requirement is defined by the vehicle chassis. At the time when this work was created a simplified design vehicle study was available. For this reason, component deployment may occur during futher development. Placement of the front suspension, the design of the front fender, or the position of the seat can influence the door mechanism design.

Figure 3.6 illustrates a simplifying marginal model (red color) for positioning body mechanism points. For ease of handling with the assembly, elements unrelated to the door mechanism have been removed. This significantly reduced the size of the assembly and have not caused a high CPU load.

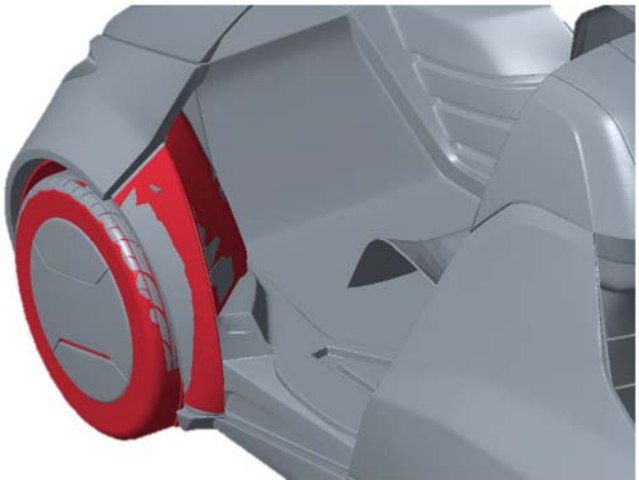

Fig. 3.6: Marginal chassis model (red)

3.2.3 DOOR MECHANISM

Requirements for the proposed mechanism:

- fully automatic system
- use of actuator
- predetermined attachment points
- determined boundaries of door movement
- lightweight design
- reliability according to user requirements
- compact packaging
- low cost

3.2.4 ELECTRONICS

Electronics for door mechanism system includes both hardware and software to ensure reliable system operation. The lithium-ion battery with a capacity of 10-15kWh and a nominal voltage of 360V is the energy source of the vehicle. Parameters of the power source serve to specify a suitable actuator.

3.3 FUNCTIONAL SAFETY ANALYSIS

Functional safety analysis is based on the functional behaviour of the item. From the perspective of the producer the priority is to resolve any dangerous situation already at an early stage of development and to propose measures to prevent malfunctions and accidents.

3.3.1 SITUATION ANALYSIS

The operational situations and operating modes (during safety life cycle) in which malfunctioning behaviour of an item will result in a hazardous event are described for both cases: when the vehicle is correctly used and when it is incorrectly used in a forseeable way. The most important situations that may arise are ranked among the highest priorities:

- door injures a pasanger during the closing process,

- door will open without passenger's command,

- passenger can not open the door (inside/ outside situation).

3.3.2 HAZARD IDENTIFICATION

The hazardous events are determined for relevant combinations of operational situations and hazards. The consequences of hazardous events are identified in the attachment.

3.3.3 CLASSIFICATION OF HAZARDOUS EVENTS

All hazardous events identified shall be classified, except those that are outside the scope of ISO 26262.

3.3.4 DETERMINATION OF ASIL AND SAFETY GOALS

Automotive Safety Integrity Level (ASIL) is a risk classification scheme defined by the ISO 26262 - Functional Safety for Road Vehicles standard. The ASIL range from ASIL D, representing the highest degree of automotive hazard and the highest degree of rigor applied in the assurance the resultant safety requirements, to QM (quality management, note: sometimes it is named as ASIL F), representing application with no automotive hazards and, therefore, no safety requirements to manage under the ISO 26262 safety processes. The intervening levels are simply a range of intermediate degrees of hazard and degrees of assurance required. [14]

Safety goals solve potential problems and define important design precautions. As part of this work, safety goals are mentioned, but they do not go into absolute detail. It is recommended to create a detailed design and process FMEA (Failure Mode and Effects) Analysis.

3.4 DESIGN SPECIFICATION

This chapter focuses on the choice of suitable concept for application to vehicle Uniti with respect to the use of available components. Created assemblies of individual concepts are grouped into basic packeting. These simplified assemblies use kinematic contstraints to enable visual analysis to verify door movement relative to the vehicle and its surroundings.

3.4.1 COMPONENT SELECTION

Torsional springs

Torsion springs utilize kinetic energy accumulation. The use of springs for door mechanism system propulsion would be particularly suited to noise and costs perspective. The use of torsion springs in Uniti is inappropriate in view of the space possibilities and the definition of the door movement.

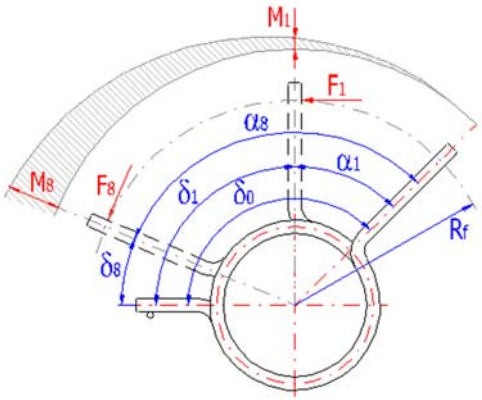

Fig. 3.7: Torsional spring schema [15]

Rail system

Linear rail system is often used for part guidance of CNC machines. In the case of controlling the rotational movement there can be curved rails. These rail systems are compact and, due to the use of bearings, they have a high load bearing capacity and rigidity. When the rider moves along the track, they do not produce significant noise. For more sophisticated applications, they are usually integrated with the Atuator into a single unit for numerically controlled operations.

Fig. 3.8: CNC rail kit [16]

Linear actuators

There are several types of linear actuators on the market. The most common actuators are electric, hydraulic and pneumatic type. When using a pneumatic actuator, a compressed air reservoir is needed, which needs to be replenished. During its operation, gaseous media escapes, causing considerable noise unacceptable for use in the Uniti vehicle. Hydraulic system can develop high forces. However, the use of the hydraulic system is costly and maintenance-intensive, mainly due to the leakage of the system. Due to the availability of electric power source in the vehicle, using of an electric actuator is the most meaningful. Electric actuators can produce high forces, have acceptable installation options and can be easily regulated.

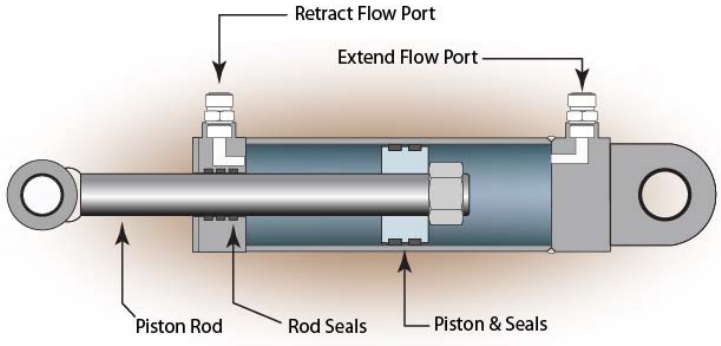

Fig. 3.9: Description of hydraulic actuator [17]

Gear

Gearing can be used primarily for the use of a suitable transmission. Thanks to the conversion, the actuator requirements related to load capacity can be reduced. By using of technical plastics, low weight and good noise and corrosion properties can be achieved. The disadvantage of toothed gear is higher system cost and more complex production.

Fig. 3.10: Plastic gearing [18]

Gas spring

„A gas spring is a type of spring that, unlike a typical metal spring, uses a compressed gas, contained in a cylinder and compressed by a piston, to exert a force. Common applications include automobiles (where they are incorporated into the design of struts that support the weight of hatchback doors while they are open) and office chairs. They are also used in furniture, medical and aerospace applications." [19]

Gas springs have compact dimensions, quiet running and affordable price. However they need an external power supply when they are in a binomial motion.

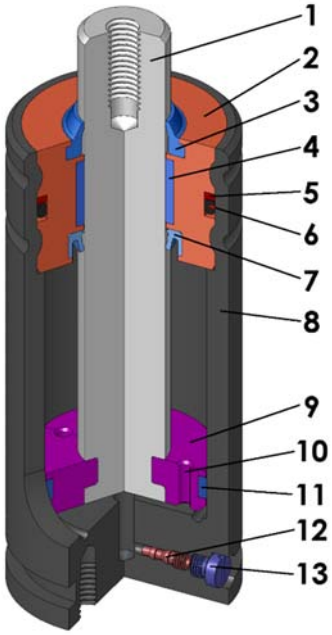

Fig. 3.11: Gas spring with sectional view: 1. Piston rod 2. Head cap 3. Piston rod wiper 4. Piston rod guide bushing 5. Retaining ring 6. O-ring 7. Piston rod seal 8. Cylinder 9. Piston 10. Flow-restriction orifice 11. Piston guide bushing 12. Valve 13. Valve-sealing [19]

Fig. 3.12: Gas strut suitable for application in automotive industry [20]

3.4.2 CONCEPT 1

Concept 1 is based on the design used by Koenigsegg Agera. As mentioned in chapter 1.2, this proposal uses a bevel gear mechanism. Movement of the door mechanism assembly can be triggered by a linear accelerator. The deployment of the pins greatly influences the motion kinematics.

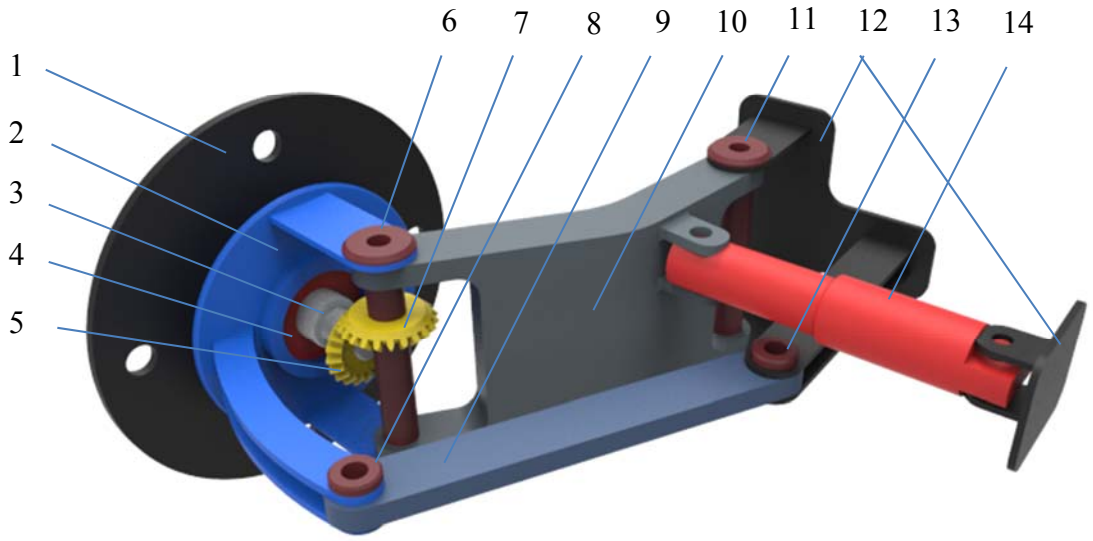

Fig. 3.13: Description of concept 1: 1.flange, 2.upright, 3.shaft, 4.bearings, 5.gear 1, 6.pin 1, 7.gear 2, 8.pin 4, 9.rod, 10.arm, 11.pin 1, 12.chassis, 13.pin 2, 14.linear actuator

To create a functional model of the moving assembly it was required to meet a number of degrees of freedom taken by individual bonds between components. This is based on the shape Kuzbatch critetion:

$$M = 6(n_L - n_J - 1) + \sum f_i \qquad (1)$$

where:

n_L…number of links
n_J…number of joints
$\sum f_i$…total degrees of freedom of all joints
M=0 proper constraint
M<0 over-constraint
M>0 under-constraint

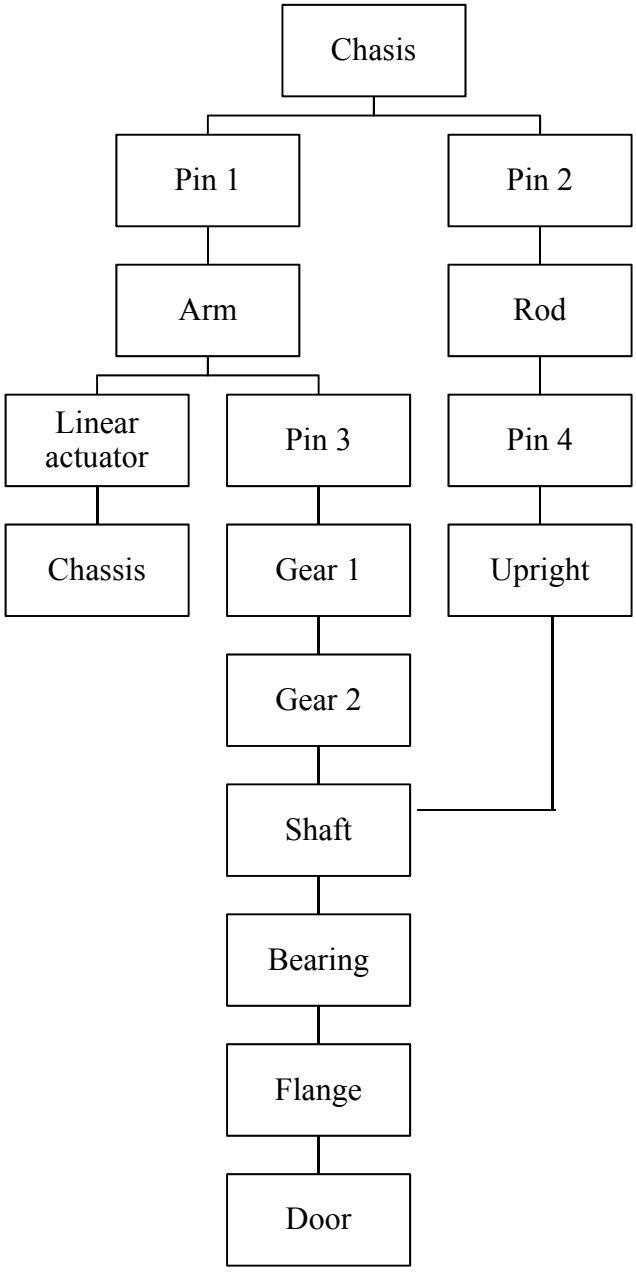

Fig. 3.14: Layout of used kinematics constraints between components of concept 1

By using kinematics contstraints: pin, cylinder, rigid was created an assembly enable movement. Between components *gear 1* and *gear 2* there was applied *Gear pair* connection. This allows mutual interaction of the two bodies in the assembly. Without defining this function, the desired motion mechanism would not be possible.

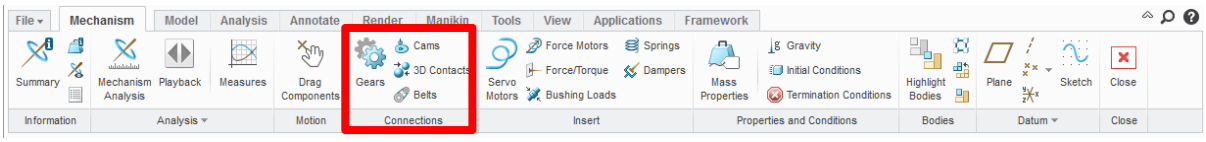

Fig. 3.15: Highlighted function Gears in software PTC Creo Parametric

Figure 3.16 shows the location of concept 1 assembly in the chassis boundary conditions with respect to the location of the door mechanism in the vehicle. In terms of packaging the linear actuator represents the biggest issue.

Fig. 3.16: Placement of concept 1 (red) into chassis boundary model

Advantages:

- rotation and translation is possible by using a single actuator,
- rigid system,
- simple control of door movement.

Disadvantages:

- concept does not fulfil motion requirements,
- patented solution,
- larger space requirements,
- required different door design,
- concept consists of many components,
- bevel gear pair is required.

3.4.3 CONCEPT 2

The second concept deals with vertical movement similar to LSD door. In this assembly, a single, linear actuator is considered to control the entire assembly motion. The positions of the pins and the length of the individual arms significantly affect the movement of the door. The 3D sketch tool was used to set the position of individual component with respect to the door trajectory.

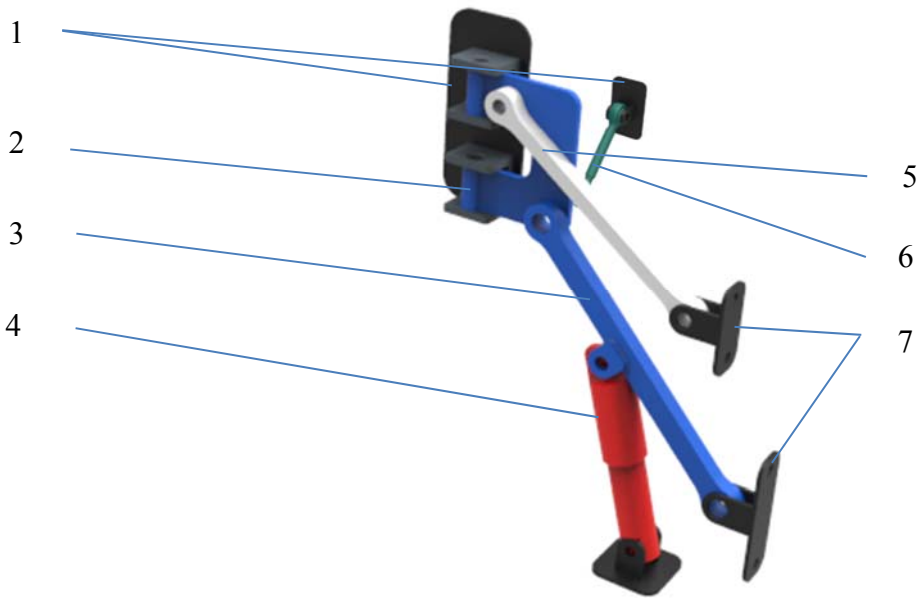

Fig. 3.17: Description of concept 2: 1.chassis, 2.vertical hinge, 3. upper arm, 4.actuator, 5. lower arm, 6.auxiliary member, 7.door attachment

Vertical hinge is attached to chassis. Two holes for upper and lower arm attachment are formed on the vertical hinge component. A point has been found on the upper arm, around the other point (on the body flange), which creates an almost circular path in motion. This auxiliary member is attached to both parts (chassis and upper arm) by two ball contstraints. This results in trajectory that does not collide with the vehicle bodywork while the door moves upward to the desired position. When using the auxiliary arm there can be used only a single linear actuator which is attached to the lower arm. Both arms are connected to attachment points on the door.

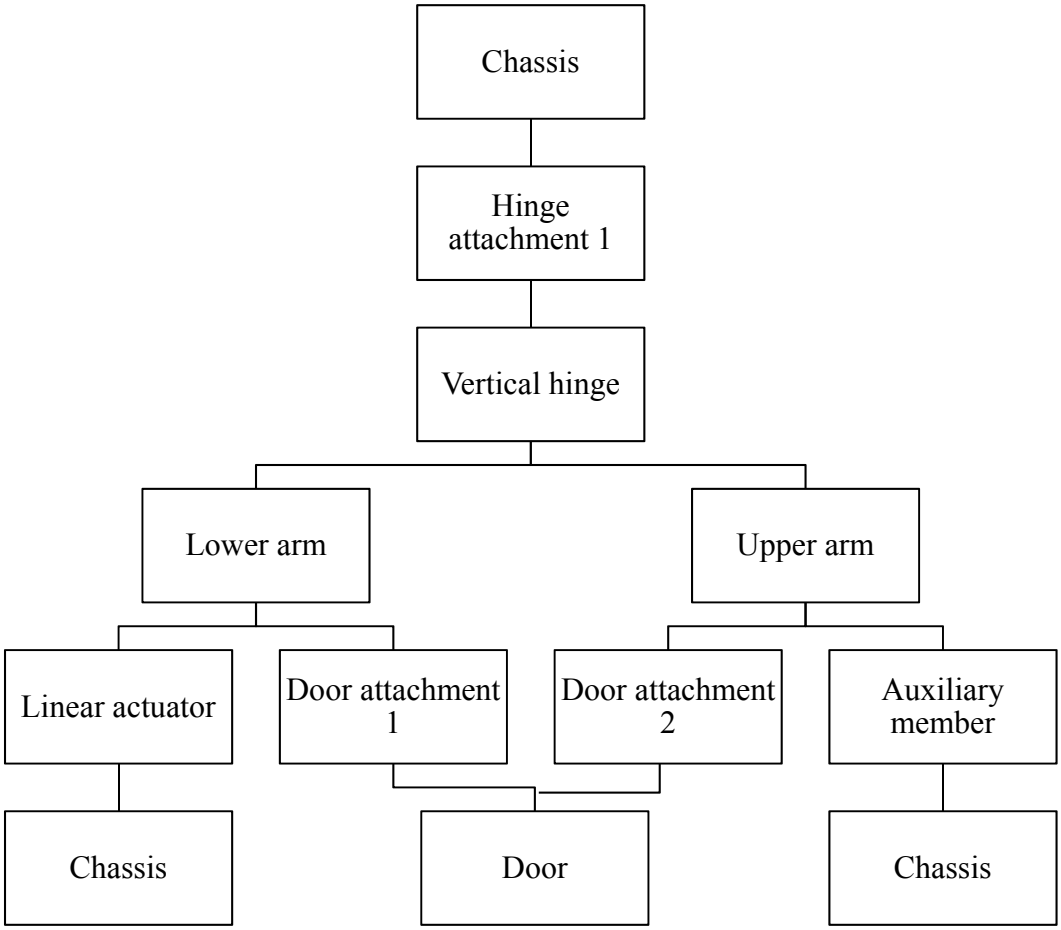

Fig. 3.18: Layout of used kinematics constraints between components of concept 2

Advantages:

- compact packeting,
- simple component design,
- use of the single linear actuator.

Disadvantages:

- door motion does not fulfil user´s expectations,
- requirement for long travel linear actuator.

Fig. 3.19: Placement of concept 1 (red) into assembly

3.4.4 CONCEPT 3

The third concept is based on Toyota's style door mechanism. Motion is divided into two separate movements. Unlike the two systems mentioned above, this proposal includes 2 actuators. The first actuator generates a translational motion. By using the second actuator the door is rotated around the axis of the front wheels. This motion fulfils user expectations.

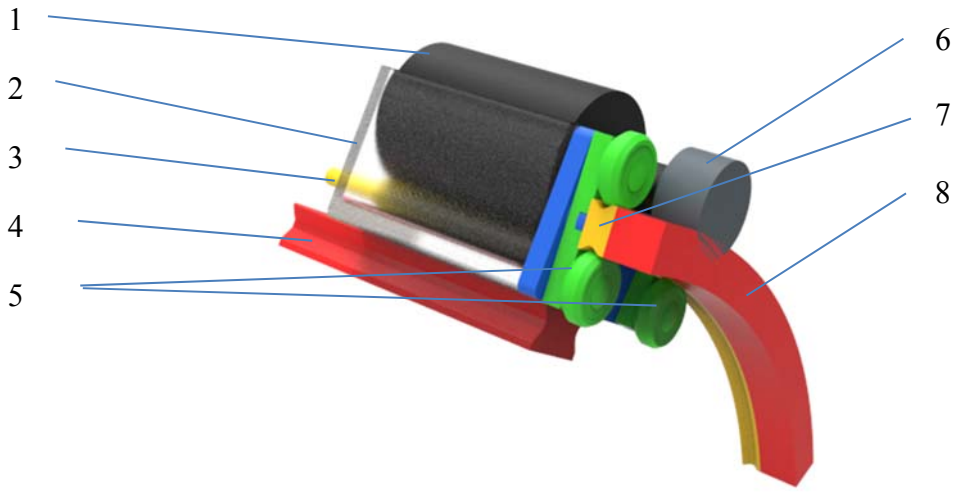

Fig. 3.20 Description of concept 2: 1.rotary actuator, 2.actuator housing, 3.linear actuator, 4.linear rail system, 5.guiding element, 6.pinion, 7.curved rail, 8.curved gear rack

The principle of this concept is the use of two rail systems and two actuators. The linear rail system is attached to the chassis. Actuator housing is connected with linear actuator, actuator housing, rotary actuator and curved rail rider. These components move together along the linear rail. The pinion is connected to the rotary actuator and is in contact with the curved rack. Curved rail and curved rack are rigidly attached to the door.

In the first phase of the motion, the mechanism is pushed out to the side. Then a rotary actuator is activated. By using gear ration it develops sufficient force to move the door. The door moves along the trajectory defined by curved rail.

Fig. 3.21: Concept 3 packating

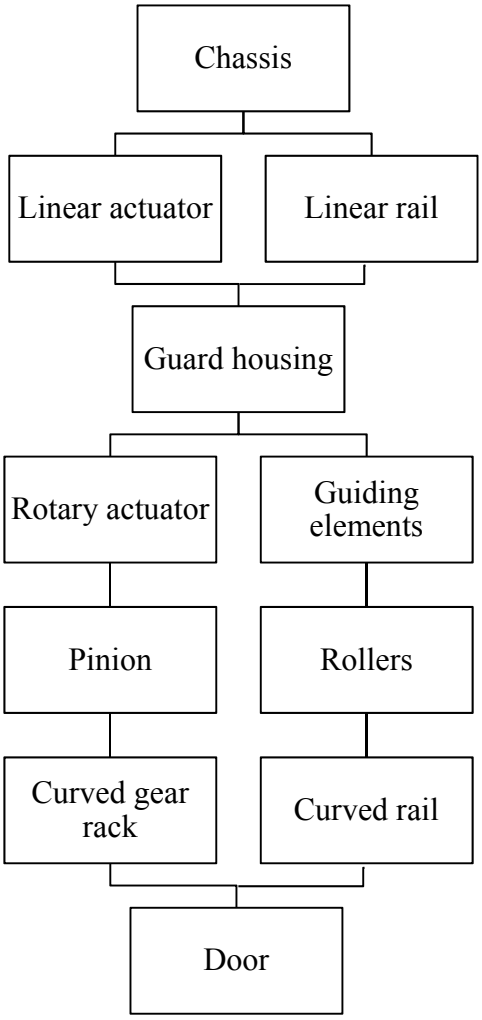

Fig. 3.22: Layout of used kinematics constraints between components of concept 3

Contrary to the first concept, tooth geometry is not required to verify door movement and create the packing of components. Thus, the pinion model is represented by cylindrical elemtent and a curved rack has been created as a rectangular profile extended along the curved trajectory.

Advantages:
- fulfils motion requirements
- compact packeting
- rigid system
- most of the components are available on the market

Disadvantages:
- use of two separated actuators
- large moment of inertia
- required curved gear rack

3.4.5 VERIFICATION OF THE DOOR MOTION

Modern developing methods include virtual reality modules. With this module, a designer or user can visualize vehicle parts and simulate their behavior. The hardware of the Uniti Kepler Pod v 1.3 simulator includes virtual reality simulator glasses and multifunction steering wheel. In the software environment, the user can see a real scale interior of the vehicle. A big advantage is the use of virtual reality in a desicion making process. In addition, the simulator is successfully used for presentation purposes.

The door movement was analyzed using this simulator. According to subjective judgment, it was decided to focus on further development of concept 3.

Fig. 3.23: Virtual Reality Simulator – Uniti Kepler Pod v 1.3

3.5 KINEMATIC ANALYSIS

Based on user requirements the most suitable velocity characteristic for linear and rotary motion was selected. Kinematic analysis is performed in MS Excel. Obtained kinematic data has been imported to the software PTC Creo Parametric to vizualize the movement of the selected assembly. Figure 3.24 illustrates the time duration of two separated door movement processes.

Fig. 3.24: Timeline of the Uniti door motion

3.5.1 KINEMATIC ASSEMBLY

This chapter describes a procedure of creating an assembly containing kinematic links, including virtual motors. Virtual motors use imput data elicted from kinematic analysis. This assembly is established in software PTC Creo Parametric and it will serve for verification of component design and collision control.

The selected assembly of concept 3 has been modified and divided into six major subassemblies: chassis, linear rail, linear actuator, door mechanism unit, two curved guinding elements, door. These elements are interconnected by using kinematic conststraints. Figure 3.25 shows the relationship between used elements. Models represented by the chassis, linear rail and linear actuator are fixed to global coordinate system *CSYS*.

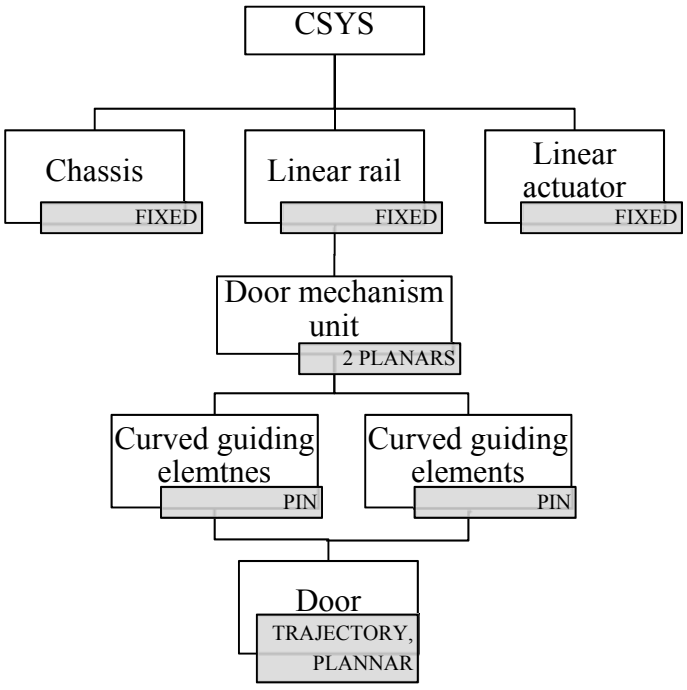

Fig. 3.25: Diagram of the kinematic assembly

Subassembly *Door mechanism unit* consists of actuator housing, rotary actuator, pinion, and rotor of linear actuator. By using of two planar connections between rail and door mechanism unit there was achieved 1 degree of freedom along rail axis.

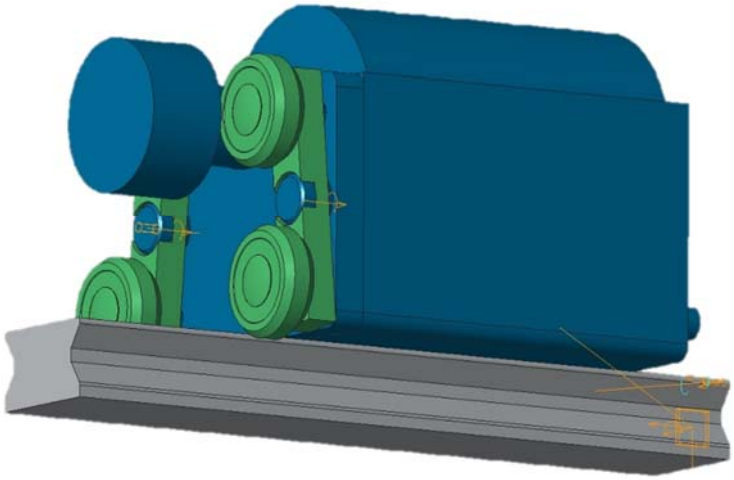

Fig. 3.26: Detailed view on section of kinematic assembly

The door mechanism unit is connected with two separated curved guiding elements. Each guiding element has one defree of freedom (rotation). The next step was to create an auxiliary point P_{01} in the center of the guiding element. This auxiliary point is shown in two planes (xy, yz) in Figure 3.27.

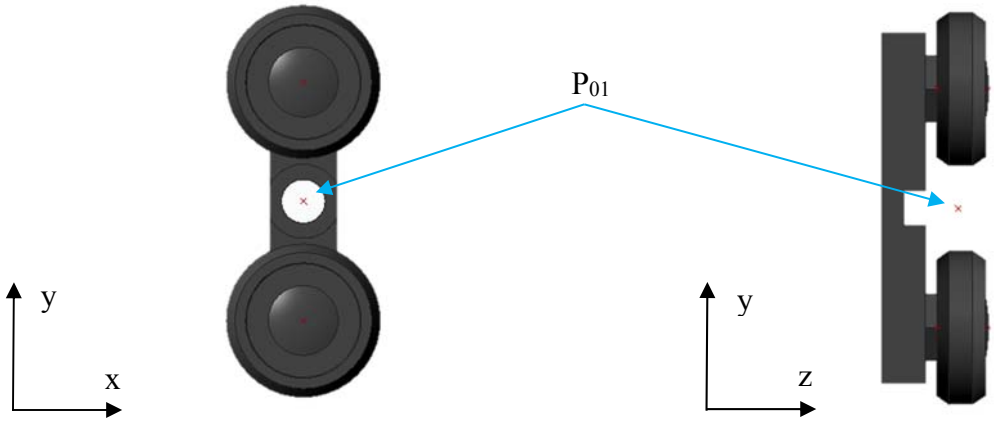

Fig. 3.27: Illustration of an auxiliary point P01 on the guiding element

Subassembly *door* consists of door model, curved rail and simplyfied curved gear rack. Curved gear rack and rail are rigidly connected with door. The connection between the curved rail and the guiding elements plays an important role. To resolve the motion of the assembly after the trajectory, a 2D trajectory sketch was created. The trajectory is shown in Figure 3.28.

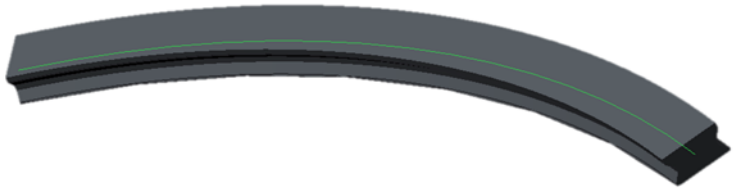

Fig. 3.28: Trajectory sketch (green) created in the middle of curved rail component

Connecting the points on each of the two guide elements with the sketch resulted in controlled door motion along defined trajectory. The last constraint between curved guiding elements and door was a plannar connection, which is parallel to the longitudinal plane of the vehicle. The doors thus have limited movement along the trajectory of the sketch while allowing movement with one degree of freedom.

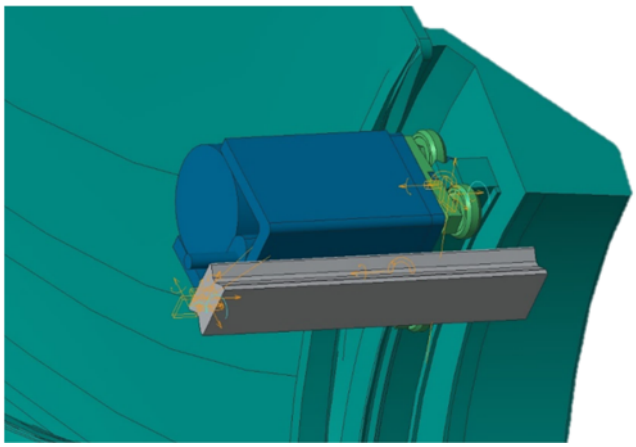

Fig. 3.29: Detailed view on kinematic assembly

Fig. 3.30: View on kinematic assembly including vehicle bodywork

After placing the components and creating kinematic contstraints, work continued on the tab *Applications – Mechanism*. This function allows to perform position, kinematic or dynamic analysis of prepared assembly. Users can also simulate springs, damers, belts, gears or detect problems with interferences and clearence. One of the biggest benefit is faster process of prototype development. [21]

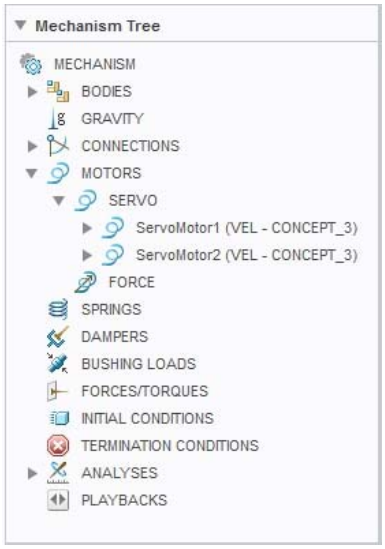

Fig. 3.31: Mechanism tree in software PTC Creo Parametric

In the mechanism tree it is possible to define motors. The servo motor can be defined by position, velocity or acceleration. The force motor can be used for a dynamic analysis. Input parameter for the force motor is a definition of force applied on components.

The next step in kinematic analysis is to find out the necessary input parameters for virtual motors.

3.5.2 KINEMATIC CHARACTERISTICS

This chapter focuses on the description and analysis of kinematic parameters of the door system. The input for kinematic analysis was velocity characteristic of door's CoG in time domain. Continuous non-linear velocity, angular velocity curve with minimum values of acceleration, angular acceleration have led to the application of modified probability density function. This function is applied to translational and rotational door movement. By using the coefficients C_1, σ_1, μ_1, the velocity curve was selected with respect to the 2 seconds time interval and total distance of 100mm.

$$v_1(t) = \frac{C_1}{\sigma_1\sqrt{2\pi}} e^{-\frac{(t-\mu_1)^2}{2\sigma_1^2}} \tag{2}$$

where:
C_1=675
σ_1=6
μ_1=1

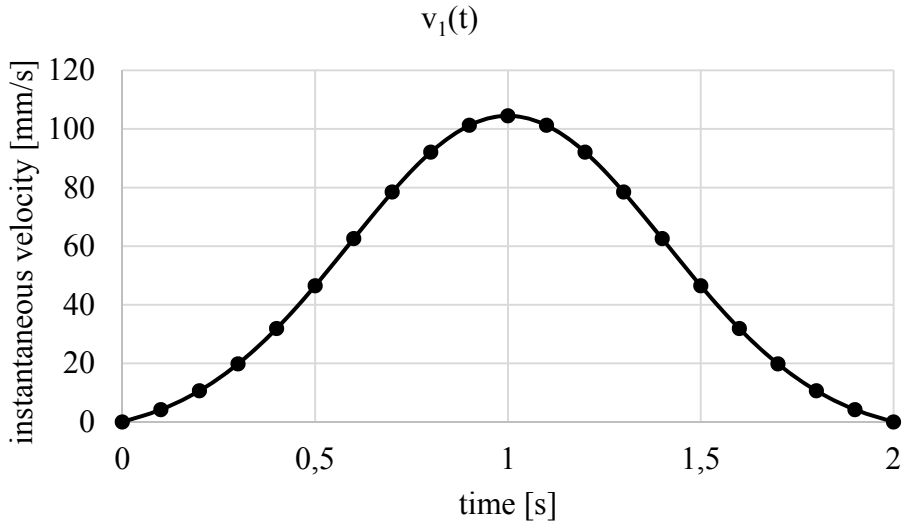

Fig. 3.32: Instantaneous velocity characteristic for translation movement

By using a numerical integration (trapezoidal method) of instantaneous velocity, it is possible to express distance characteristic:

$$s_1(t) = \int v_1(t)dt \tag{3}$$

The characteristics of instantaneous acceleration was achived by numerical derivation of instantaneous velocity.

$$a_1(t) = \dot{v_1}(t) \tag{4}$$

During rotational door movement there is 60 degrees rotation required in the time interval of 3 seconds. The angular velocity ω_1 characteristics is similar to the velocity of door translation.

$$\omega_1(t) = \frac{C_2}{\sigma_2\sqrt{2\pi}} e^{-\frac{(t-\mu_2)^2}{2\sigma_2^2}} \tag{5}$$

where:
C_2=196
σ_2=3
μ_2=1,5

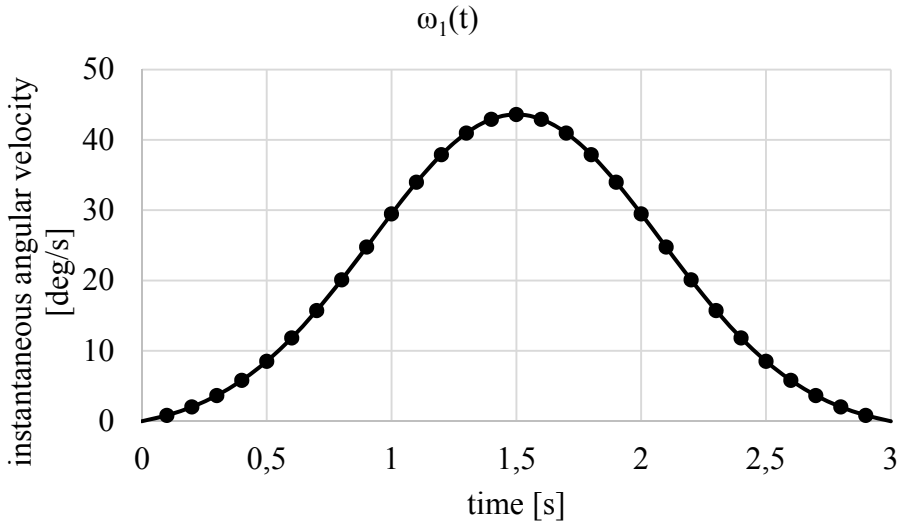

Fig. 3.33: Instantaneous angular velocity characteristic for rotational movement

By using a numerical integration of instantaneous angular velocity ω_1, it is possible to express angle characteristics φ_1.

$$\varphi_1(t) = \int \omega_1(t)dt \tag{6}$$

The characteristics of instantaneous angular acceleration α_1 was achived by numerical derivation of instantaneous angular velocity.

$$\alpha_1(t) = \dot{\omega_1}(t) \tag{7}$$

During the numerical integration process errors arise but have not been considered for this application.

Characteristics of the instantaneous velocity and instantaneous angular were imported into the PTC Creo Parametric environment and used as inputs for two virtual motors: *Servomotor 1, Servomotor 2*. The adjustment process is shown in the figure 34.

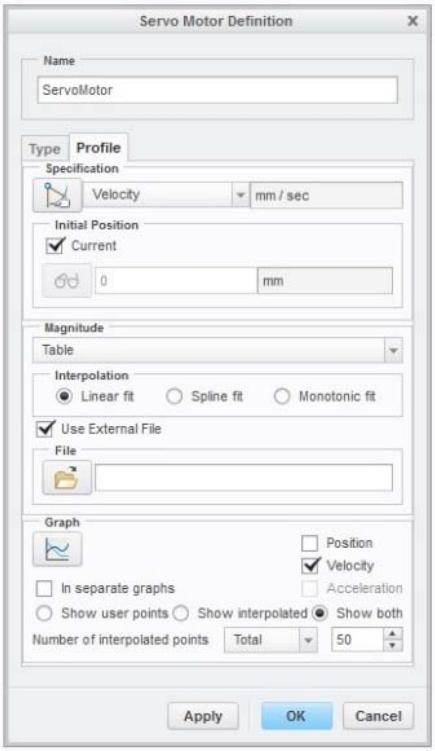

Fig. 3.34: Servo motor definition window

Servomotors operate at a different time interval. Servomotor 1 is actuated in interval 0-2s, servomotor 2 operates in interval 2-5s. This command was set in the *analysis definition* window.

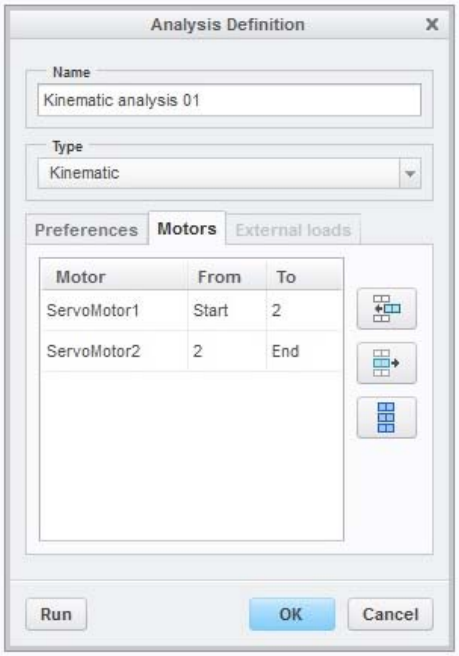

Fig. 3.35: Analysis definition window

During this analysis several collisions were detected. After several iterations the final position of components was set. In this process, the advantage of the creo parametric environment was demonstrated.

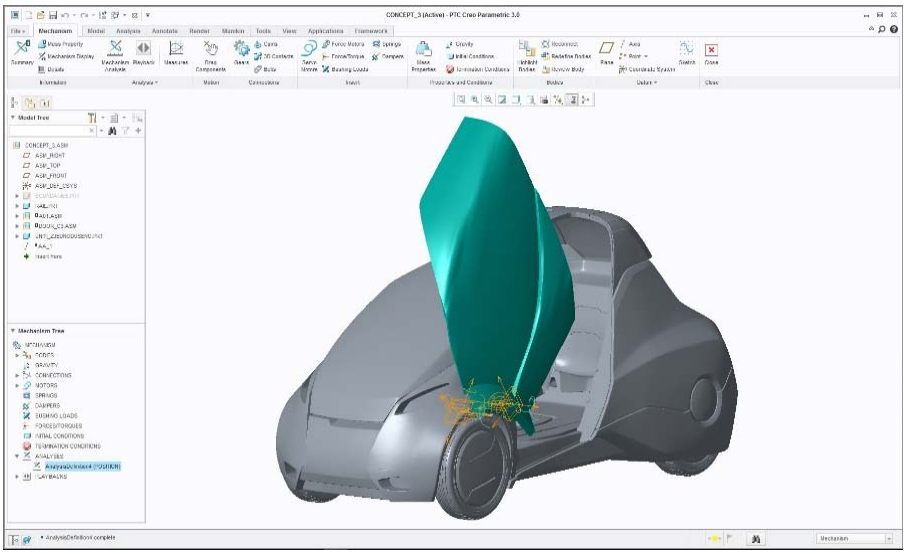

Fig. 3.36: Final kinematic assembly of door mechanism in PTC Creo Parametric enviroment

In the *table 4* there are given the most important kinematic parameters of the proposed system. All kinematic characteristics are attached in the appendix of this thesis.

Tab. 3.4: Maximal kinematic values

	Kinematic parameters of door CoG	Symbol	Value
Translational movement	Maximal distance	s_1	100 mm
	Maximal instantaneous velocity	v_1	104,49 mm/s
	Maximal instantaneous acceleration	a_1	0,16 m/s^2
Rotational movement	Maximal angle	φ_1	60 deg
	Maximal instantaneous angular velocity	ω_1	43,60 deg/s
	Maximal instantaneous angular acceleration	α_1	47,2 deg/s^2

3.6 DYNAMIC ANALYSIS

Dynamic analysis is based on the detected kinematic values (acceleration, angular acceleration) of door cog (center of gravity). The aim of this dynamic analysis is to determine the power and energy requirements for the choice of suitable actuators. Various operating states that may affect the function of the system will also be considered in this part of thesis. This chapter does not consider losses caused by friction.

3.6.1 DOOR MOVEMENT

The greatest load on the system is expected during the door opening process. The process of opening and closing the door is solved in two separated steps. In the first step only the translation door motion is considered. In the second step the rotational motion is analyzed.

Translation

The solution for translational dynamics is based on Newton's second law of motion. Where m_{DOOR} represents constant door weight and a_1 is a variable value of door CoG acceleration in time interval 0-2seconds.

$$F_1(t) = m_{DOOR} \cdot a_1(t) \tag{8}$$

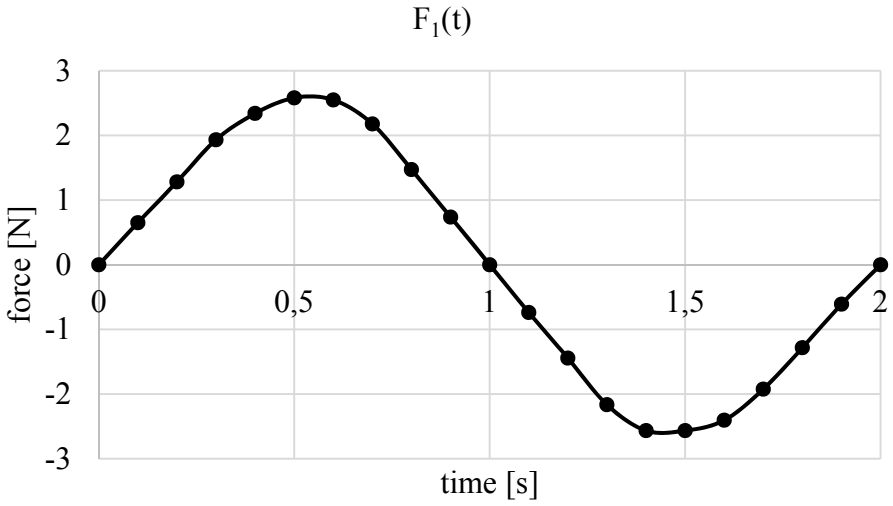

Fig. 3.37: Force characteristics during translation motion:

Following equations 9,10 determine performance and work characteristic during the translational process.

$$P_1(t) = F_1 \cdot v_1 \tag{9}$$

$$W_1(t) = \int P_1(t)dt \tag{10}$$

The maximum values of the parametre found within translational motion are presented in table 5.

Rotation

The analytical method was chosen to calculate loading conditions during door rotation. Rotational dynamic equation is used to describe the numerical model.

An equation 11 includes the effect of gravity force as well as angular acceleration acting on the center of gravity. As in the previous step a constant value of door weight m_1 is considered. The distance between the door cog and the axis of rotation is indicated by constant d_1. Parameter φ expresses the angle of door rotation relatively to ground. Moment of door inertia I_z reffered in center of gravity must be in formula modified by the Parallel axis theorem (Stainer's formula). When the door is closing, the direction of angular acceleration changes. For this reason there is used operator ± in equation. All parameters are illustrated in figure 3.38.

$$M_1(t) = m_1 \cdot g \cdot d_1 \cdot cos(\varphi) \mp \left(\left(I_z + m_1 \cdot {d_1}^2\right)\right) \cdot \alpha_1(t) \qquad (11)$$

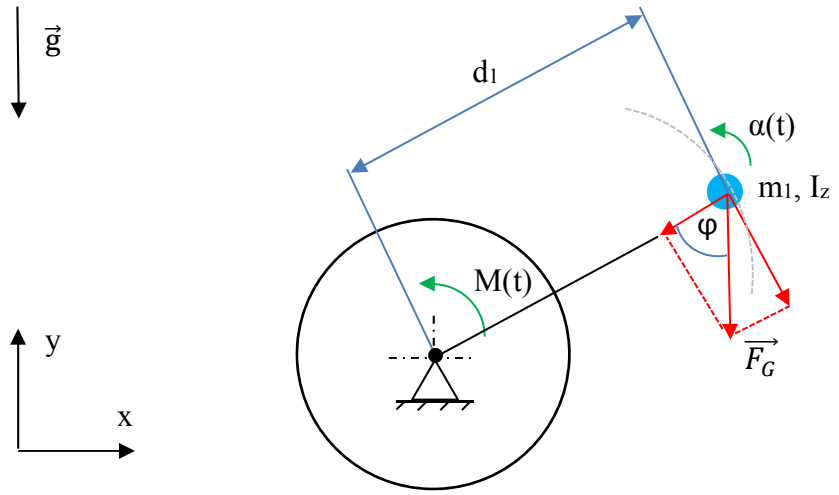

Fig. 3.38: Illustration of door opening situation

The graph shown in figure 3.39 represents the situation of opening the door in the time interval (0;3)s and simultaneously closing the door in the time interval (3;6)s.

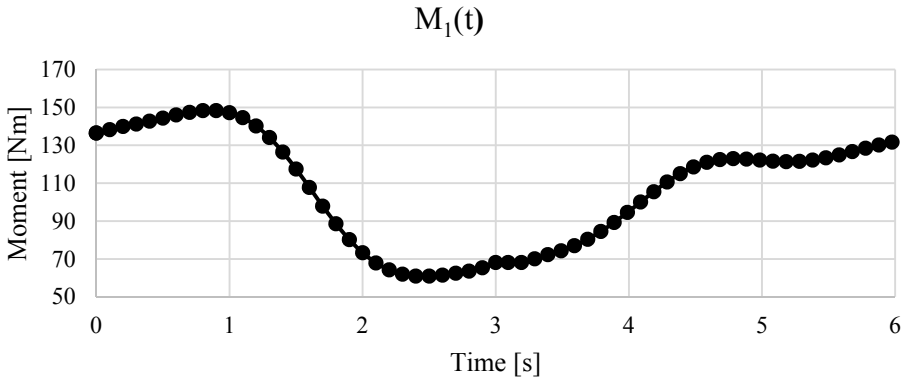

Fig. 3.39: Moment characteristic during opening and closing process

Another key parameter to determine the appropriate actuator is performance. By using values calculated in previous steps: moment M_1 and angular velocity ω_1, required performance of rotary actuator was determined in equation 12:

$$P_2(t) = M_1\omega_1 \tag{12}$$

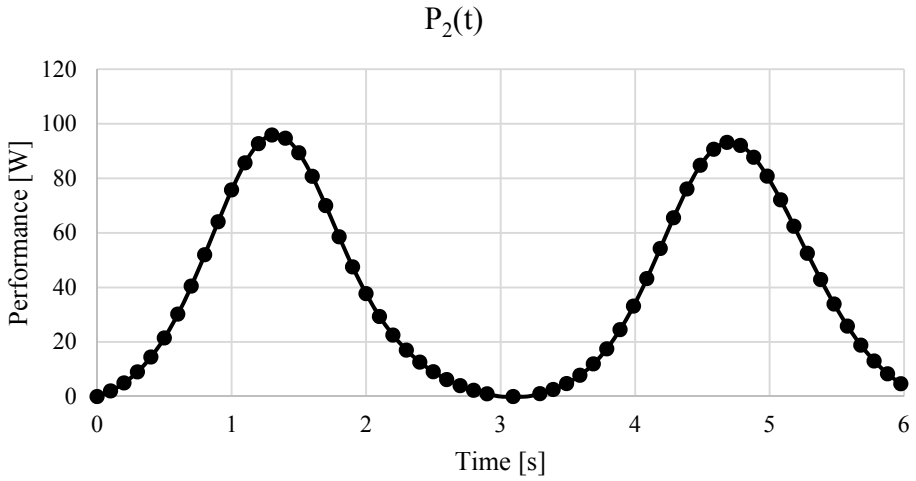

Fig. 3.40: Performance characteristics during opening and closing process

In terms of energy parameter work for door opening and closing process was also expressed within a dynamic analysis.

$$W_2(t) = \int P_2(t)dt \tag{13}$$

Tab. 3.5: Maximum dynamic values

	Dynamic parameter	Symbol	Value
Tranlational movement	Maximal force	F_1	2,58N
	Maximal performance	P_1	0,17W
	Total energy (1 cycle)	W_1	0,32J
Rotational movement	Maximal moment	M_1	148,3Nm
	Maximal performance	P_2	95,8W
	Total energy (1 cycle)	W_2	237J

3.6.2 AERODYNAMIC FORCE

During the use of the vehicle, there may be a situation in which the wind will act on the surface of open door. This can cause an aditional load which could damage the mechanism. For the determination of this magnitude it was necessary to specify an upper limit to which the mechanism must withstand.

The Beaufort wind force scale is an empirical measure that relates wind speed to observed conditions at sea or on land. For maximal wind force was choosen a gale. On the scale there is gale number eight out of twelve. Its wind speed v_2 is defined up to 20,7 m/s. This wind strength can break tree branches, walking in the wind it is almost impossible. In extreme cases it can break down roofs or chimneys.[22] To calculate the force developed by wind acting on the open door surface, Bernoulli equation has been used:

$$\frac{1}{2}\rho \cdot {v_2}^2 + p + \rho \cdot g \cdot h = Constant \tag{14}$$

Where ρ is the density of the fluid at all points in the fluid, v_2 is the fluid flow velocity at a point a streamline, p is pressure at choosen point, h is the elevation of the point above a reference plane.

For further calculation there was used a part of equation which comprises only a portion of the kinetic energy. Fluid (air) density ρ was selected 1,29kg/m^3.

$$p = \frac{1}{2}\rho \cdot v_2^2 \tag{15}$$

$$p = \frac{1}{2} \cdot 1{,}29 \cdot 20{,}7^2 = 276{,}36\ Pa \tag{16}$$

The calculation is simplified to a state where the fluid pressure p is perpendicular to the open door area without affecting the turbulent flow. It is important to verify loads from both door sides. Therefore this load case is solved in two seperated parts: for fluid pressure applied on the right side the considered area was S_1. For the fluid pressure applied on left side, area S_2 was set. Both open door areas were measured in the CAD environment by function *Measure*, *area*.

Then the aerodynamic force F_{A1} applied on door open area from right side is defined as:

$$F_{A1} = p \cdot S_1 \tag{17}$$

$$F_{A1} = 276{,}36 \cdot 0{,}59 = 163{,}05 \approx 163N \tag{18}$$

The aerodynamic force F_{A2} applied on door area from right side is defined as:

$$F_{A2} = p \cdot S_2 \tag{19}$$

$$F_{A2} = 276{,}36 \cdot 0{,}94 = 259{,}77 \approx 260N \tag{20}$$

The aerodynamic force acts trought center of pressure. The center of pressure (CoP) is the average location of the pressure. Determination of the center of pressure is a complicated procedure because the pressure changes around the door. [23] To simplify the numerical model, the position of the center of pressure was set in the center of gravity for each side door surface S_1 and S_2 determined at maximum opening position. These points have different location and are illustrated in figure 3.41 and figure 3.42.

In the CAD model situation shown in figure 3.41, the coordinate difference in the *x* axis and the *y* axis was measured between the center of pressure and the door mechanism chassis attachment point *1*. The distance in the x-axis direction between the center of pressure and the point *1* is 37mm. This value has not been considered. An important value is the distance between points (*CoP* and *1*) in the y-axis direction. The distance d_2 is 782mm. Maximum value of the moment Mx_1 caused by aerodynamic force F_{A1} in the center of the pressure acting on the door mechanism mounting:

$$M_{X1} = F_{A1} \cdot d_2 \tag{21}$$

$$M_{X1} = 163 \cdot 0{,}782 = 118Nm \tag{22}$$

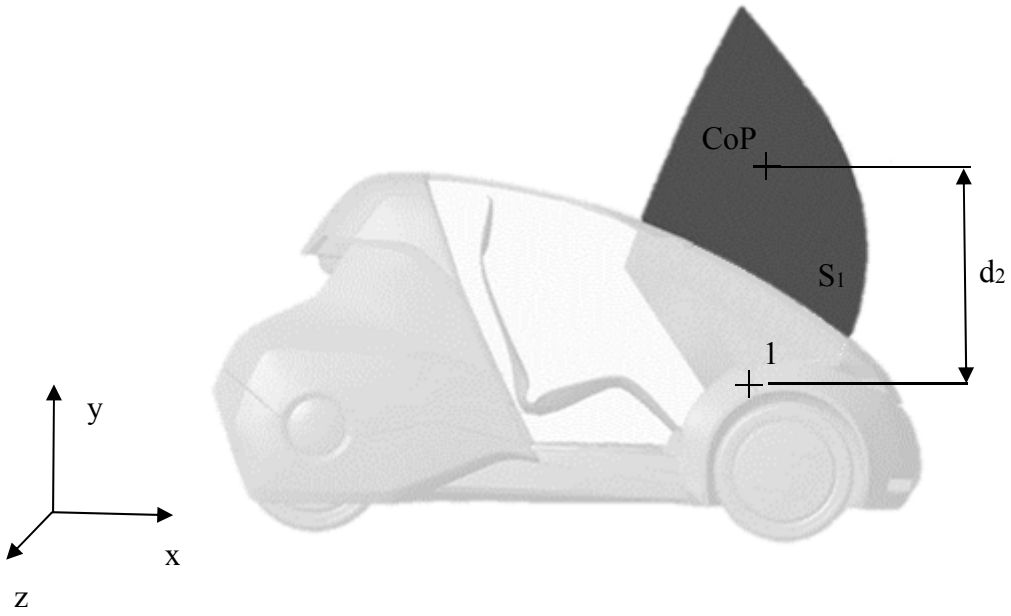

Fig. 3.41: Illustration of distance between attachment point and center of pressure applied on surface S1

The aerodynamic force can also act on the outside door surface. When door locks are unlocked, the moment generated by aerodynamic force is captured in door mechanism mounting point.

From the situation shown in figure 3.42 emerges, the maximum magnitude of moment M_Y is in door position φ_1=0deg (figure 48). The maximum momemt M_X will be achieved in fully opened door φ_2=60deg (figure 3.43). Therefore analysis consists of two separated situations.

In the first situation, the door position is defined by angle φ_1 (closed). The center of pressure has a certain position given by dimensions d_3 and d_4. The value of moment M_{X2} is defined by arm d_3 and aerodynamic force F_{A2}. The magnitude of moment M_{Y1} depends on aerodynamic force and arm d_4.

$$M_{X2} = F_{A2} \cdot d_3 \tag{23}$$

$$M_{X2} = 260 \cdot 0{,}161 = 41{,}9Nm \tag{24}$$

$$M_{Y1} = F_{A2} \cdot d_4 \tag{25}$$

$$M_{Y1} = 260 \cdot 0{,}609 = 158{,}3Nm \tag{26}$$

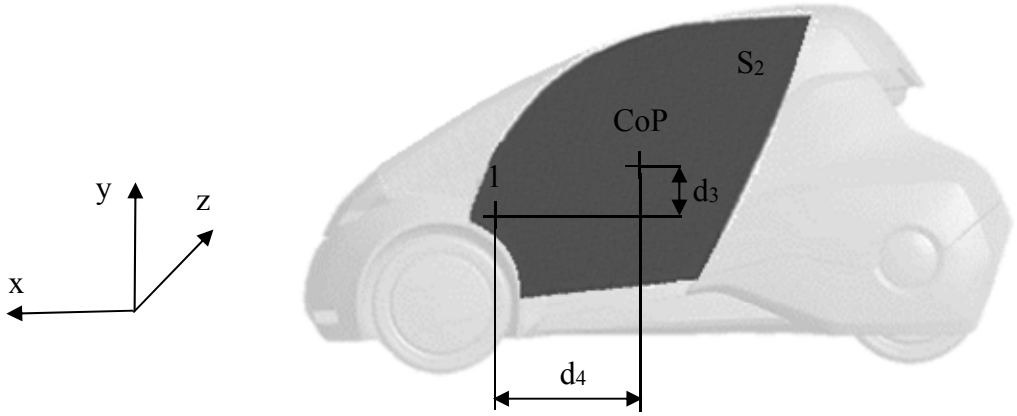

Fig. 3.42: Illustration of distance between attachment point and center of pressure applied on surface S2 (closed door position)

The second situation considers door position defined by angle φ_2 (opened). In the model situation shown in figure 3.43, the position of new center of pressure was measured again in both (x, y) axis directions from door attachment point *1*. The distance d_5 is 631mm. The distance difference between point 1 and center of pressure in x direction is 23mm. This distance difference was neglected. Moment M_{X2} caused by aerodynamic force F_{A2} applied in the center of the pressure acting on the door mechanism mounting:

$$M_{X3} = F_{A2} \cdot d_5 \tag{27}$$

$$M_{X3} = 260 \cdot 0{,}631 = 164Nm \tag{28}$$

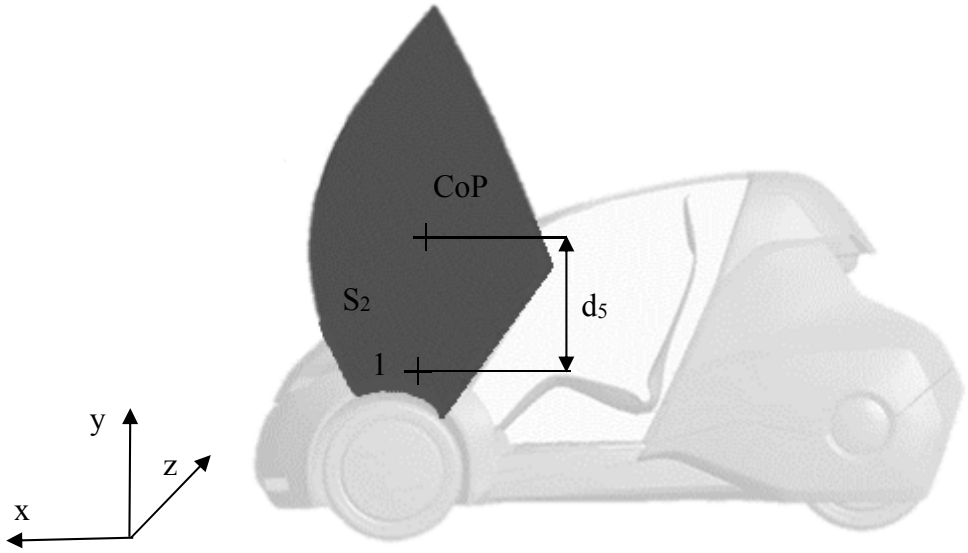

Fig. 3.43 : Illustration of distance between attachment point and center of pressure applied on surface S2 (open door position)

From observed results moment M_{X3} has the highest magnitude. With respect to the initial design of the door shape and the simplified calculation model, it is necessary to take the maximum aerodynamic force with reserve. However, values M_{X3} and M_{Y1} found by these analytic equations are useful for futher component design.

Tab. 3.6: Maximum estimated load caused by aerodynamic force

M_{X1}	118Nm
M_{X2}	41,9Nm
M_{X3}	164Nm
M_{Y1}	158,3Nm

3.7 COMPONENT DESIGN

Based on loading conditions obtained by using numerical methods in chapter 3.6, this section of thesis focuses on detailed component design. The general requirements for components include high reability and low noise level. Due to the need to use electric actuators, the noise emitted during motion is counted. However, the amplitude-frequency characteristic of the sound pressure plays a significant role in selecting the actuator. The linear actuator will be connected to DC voltage system of the vehicle.

3.7.1 LINEAR ACTUATOR SELECTION

In terms of kinematic parameters linear actuator must fulfil maximal instantaneous velocity of 105mm/s and the stroke of 100mm. Dynamic analysis in the section 3.6.1 has determined the maximum force and performance that the actuator has to develop. However, based on results of dynamic effect caused by fluid pressure applied on door surface S_2 (chapter 3.6.2), the requirements for actuator selection must be modified.

The minimum force F_{1L} which the linear actuator must develop is defined as the sum of force F_1 and maximum aerodynamic force F_{A2} applied on door surface S_2.

$$F_{1L}(t) = F_1(t) + F_{A2} \tag{29}$$

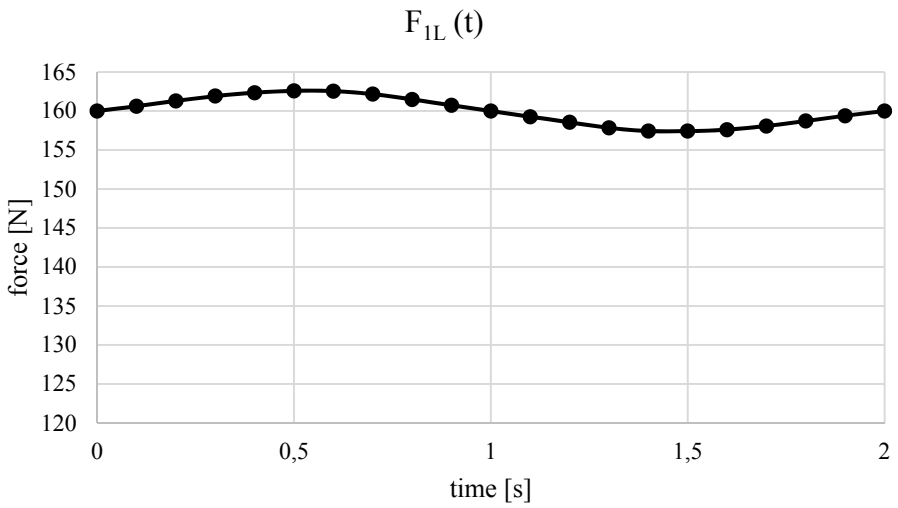

Fig. 3.44: Characteristics of force $F_{1L}(t)$

The required magnitude of linear actuator performance was set based on equation 29. The amount of mechanical work during opening process is determined by numerical integration of the performance.

$$P_{1L}(t) = F_{1L}(t) \cdot v_1(t) \tag{30}$$

$$W_{1L}(t) = \int P_{1L}(t)dt \tag{31}$$

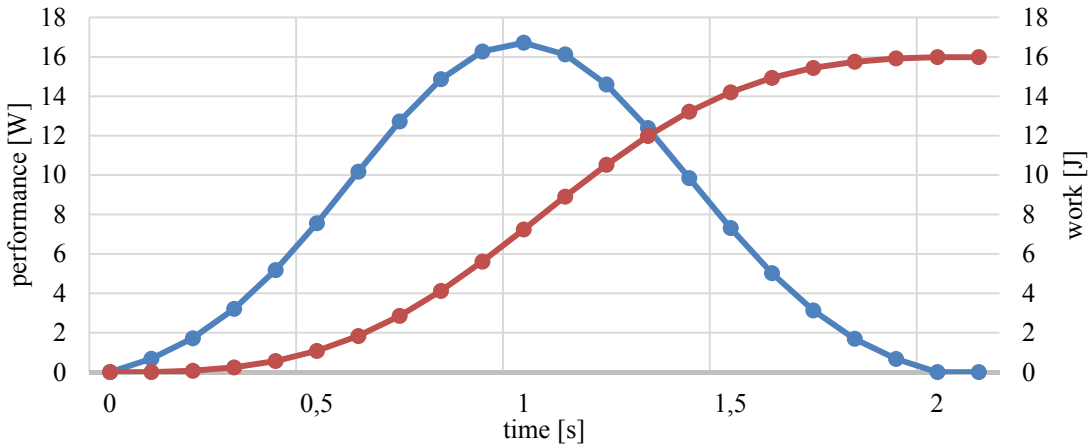

Fig. 3.45: Characteristics of $P_{1L}(t)$ – blue color, and $W_{1L}(t)$ – red color

Based on dynamic analysis, required force of linear actuator was set as 163N. The actuator must be able to develop maximal performance of 16.7W. During opening door process, the actuator performs the mechanical work of 16J. After a time interval of 2 seconds, the door position is locked. Then the actuator will not be used until the closing process. Detailed description of locks in the system is presented in chapter 3.8.

Appropriate actuator selction was based on market analysis. The LinMot's portfolio provides actuators for diferent applications. LinMot motors are electromagnetic direct drives in tubular form. The linear motion is produced purely electrically and wear-free, without any intermediate coupling of mechanical gearboxes, spindles, or belts. [24]

The linear motor consists of two parts: the slider and the stator. The slider is made of neodymium magnets that are mounted in a high-precision stainless steel tube. From the catalogue available on LinMot websites stator PS01-37Sx120F-HP-N-AGI was selected. Length of the rotor is 250mm. This type of motor is the shortest form factor for LinMot linear motors. Short motors have been developed especially for applications with limited space constraints. Within LinMot designer software, the actuator movement can be programmed. The dimensions of the product, including its characteristics, are attached in the thesis appendix.

Fig. 3.46: 3D model of the LinMot stator PS01-37Sx120F-HP-N-AGI

Tab. 3.7: LinMot PS01-37Sx120F-HP-N-AGI stator parameters [24]

Stator specification	Value
maximal stroke	1480mm
maximal velocity @48VDC	3,8m/s
maximal current @48VDC	3,8A
peak force	255N
stator mass	0,8kg

3.7.2 ROTARY ACTUATOR SELECTION

The rotary actuator must not only meet performance requirements, withstand applied loads, but must also ensure movement accuracy, posibility to control the motion and has compact dimensions due to location in the assembly. Selection of rotary actuators was concentrated on industrial-grade servomotors which can be controlled.

Based on market analysis, Teknic product portfolio has been found. The Teknic Company offers brushless rotary servomotors. The brushless servomotors have excellent acustic properties and provide sufficient performance for an application in Uniti vehicle. These Teknic servomotors include a brushless servo motor, encoder and vector servo drive in a single unit. The CPM-SDHP-3432S-ELS was selected for the servomotor control and financial cost.

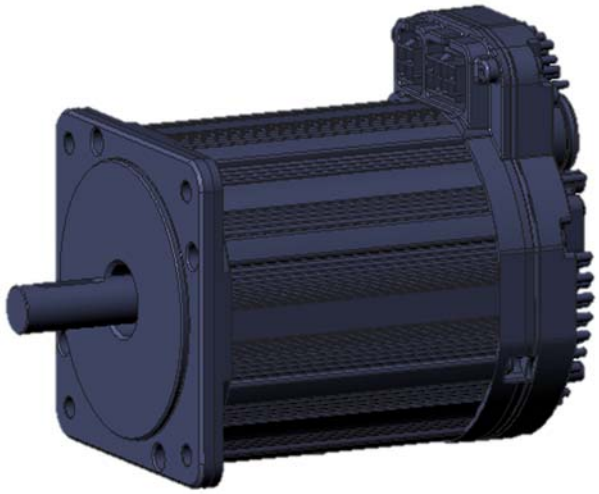

Fig. 3.47: Brushless DC servomotor CPM-SDHP-3432S-ELS

Tab. 3.8: Parameters of selected rotary actuator [25]

Servomotor specification	Value
maximal peak torque	9,85 Nm
maximal speed	1150 [1/min]
achievable resolution	0,06 deg
DC BUS voltage	75V
rotor Inertia	2,087 kg.cm^2
weight	2,81 kg

Characteristiscs of actuator have been found on supplier websites. Courses of performance and moment characteristics are shown at figure 3.48 The moment characteristics have a linear magnitude of maximum torque in range from 0 to 350[1/min]. The motor has a maximum performance of 2,03[kW]@600[1/min].

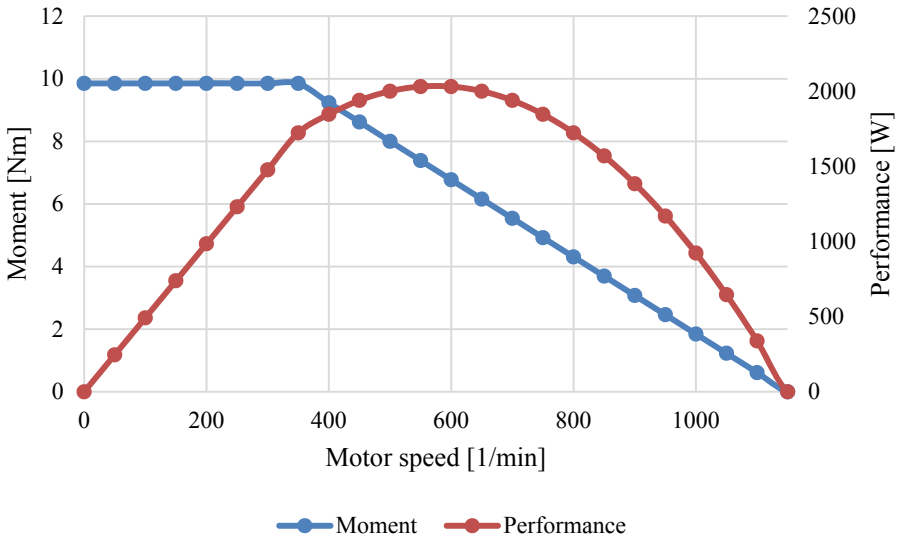

Fig. 3.48: Characterictics of the selected rotary actuator [25]

3.7.3 GEARING PROPOSAL

This chapter deals with the design of spur gearing with regard to dynamic analysis in chapter 3.6. The aim is to select a suitable gear ration between the rotary actuator and the door. It is necessary to design a geometry based on basic engineering calculations with respect to boundary conditions in assembly listed in table 8:

With respect to required moment for door rotational movement during the opening process, the choice of actuator without the use of gear ratio for application in the urban vehicle would be almost impossible. The advantage of using an electric rotary actuator is its moment characteristics. Selected rotary actuator has a maximum torque of 9.85Nm. The maximum torque required is 148.3Nm.

Tab. 3.9: Boundary conditions in door mechanism assembly

Parameter	Symbol	Value
Maximal addendum circle diameter for pinion	D_{a1MAX}	60mm
Maximal addendum circle diameter for curved rack	D_{f2MAX}	800mm
Maximal face width	b_{MAX}	50mm
Diameter of motor output shaft	D_3	12,7mm

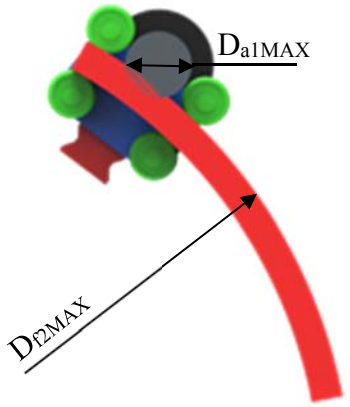

Fig. 3.49: Illustration of parameters in concept 3 assembly

$$i_{1,2} = \frac{D_2}{D_1} = \frac{z_2}{z_1} = \frac{M_2}{M_1} \tag{32}$$

where:

D_1…pitch circle diameter of drive gear [mm]
D_2…pitch circle diameter of driven gear [mm]
z_1…number of teeth on input gear [-]
z_2…number of teeth on output gear [-]

M_1…applied moment on input shaft [Nm]
M_2…applied moment on output shaft [Nm]
The first step involves selection of gear ratio. Parameters of the maximum motor moment and maximum required moment applied on mechanism have been considered into the calculation.

$$i_{1,2} = \frac{M_2}{M_1} \tag{33}$$

$$i_{1,2} = \frac{148{,}3}{9{,}85} = 15 \tag{34}$$

After the selection of gear ratio, the calculation of the maximum motor speed follows. Based on kinematic analysis maximal instantaneous angular velocity of door during opening process has been observed. This parameter is marked in equation 31 as ω_{2max}=43,61deg/s = 0,7611rad/s. Then the maximum door speed n_{2max} is:

$$n_{2max} = \frac{\omega_{2max} \cdot 60}{2\pi} \tag{35}$$

$$n_{2max} = \frac{0{,}7611 \cdot 60}{2\pi} = 7{,}27\ [min^{-1}] \tag{36}$$

Once the maximum speed of the door n_{2max} is known, it is possible to express the maximum speed of the drive gear n_{1max} using the gear ratio $i_{1,2}$:

$$i_{1,2} = \frac{n_{1max}}{n_{2max}} \tag{37}$$

$$n_{1max} = n_{2max} \cdot i_{1,2} \tag{38}$$

$$n_{1max} = 7{,}27 \cdot 15 = 109{,}05\ [min^{-1}] \tag{39}$$

The maximum motor speed that can occur during the door operations is lower than the maximum speed prescribed by the selected actuator manufacturer. By looking at the performance characteristics of the servomotor (figure 3.48), it is obvious that the range of motor speed is always in the linear region of performance and maximum moment value.

The next step is the proposal of pinion (drive gear) geometry. The size of module *m* was selected 3mm. The number of teeth z_1 of the pinion was choosen with respect to the construction and production posibilities. Parameter D_{a1} used in equation 36 expresses the addendum circle diameter.

$$m = \frac{D_{a1}}{(z_1 + 2)} \tag{40}$$

$$D_{a1} = m(z_1 + 2) \tag{41}$$

$$D_{a1} = 3 \cdot (16 + 2) = 54mm \tag{42}$$

Observed addendum circle diameter of pinion satisfy dimension requirement shown in table 8.

Calculation of the pinion pitch diameter D_1 is presented in equation 39:

$$D_1 = m \cdot z_1 \tag{43}$$

$$D_1 = 3 \cdot 14 = 48mm \tag{44}$$

In the next step is geometry of driven gear (curved rack) calculated. Curved rack pitch diameter D_2 is defined as:

$$D_2 = i \cdot D_1 \tag{45}$$

$$D_2 = 15 \cdot 48 = 720mm \tag{46}$$

To verify inslatation possibility of curved rack (driven gear) attached to door, it is required to determine the dimension of the base circle diameter D_{f2}. To determine the base circle diameter it is necessary to quantify the gear clearance c_{a1} and dedendum h_{f2} which serve as input parameters to equation 47:

$$c_{a2} = 0{,}25 \cdot m \tag{47}$$

$$c_{a2} = 0{,}25 \cdot 3 = 0{,}75mm \tag{48}$$

$$h_{f2} = m + c_{a2} \tag{49}$$

$$h_{f2} = 3 + 0{,}75 = 3{,}75mm \tag{50}$$

$$D_{f2} = D_2 + 2 \cdot h_{f2} \tag{51}$$

$$D_{f2} = 720 + 2 \cdot 3{,}75 = 727{,}5mm \tag{52}$$

Observed base circle diameter D_{f2} of curved gear rack satisfies the dimension requirements.

The most important gearing parameters are shown in table 3.10:

Tab. 3.10: Parameters of gearing geometry

	Pinion		Curved gear rack	
Parameter	Symbol	Value	Symbol	Value
Modul	m	3mm	m	3mm
Number of teeth	z_1	16	z_2	40*
Addendum circle diameter	D_{a1}	54mm	D_{a2}	712,5mm
Pitch circle diameter	D_1	48mm	D_2	720mm
Base circle diameter	D_{f1}	40,5mm	D_{f2}	727,5mm
Teeth high	h_1	6,75mm	h_2	6,75mm
Width of space	w_1	4,712mm	w_2	4,712mm
Circular pitch	P_{1P}	9,425mm	P_{2P}	9,425mm
Gear clearance	c_{a1}	0.75mm	c_{a2}	0.75mm
Face width	b_{1F}	40mm	b_{2F}	40mm
Axis distance	a_d	336mm	a_d	336mm

**number of curved gear rack which will be in contact with pinon during door movement, not number of complete gear*

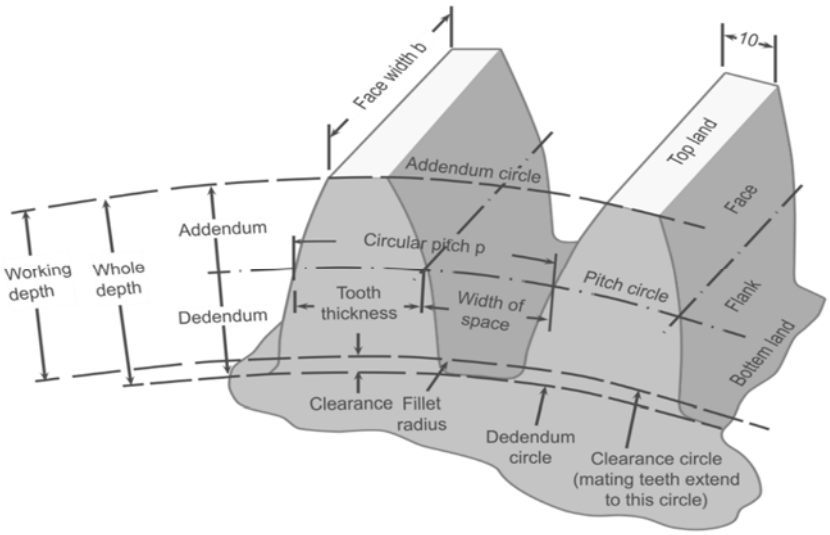

Fig. 3.50: Description of spur gear parameters [26]

Attempts to reduce mechanism weight and noise level during door movement did not avoid gearing design proposal. When gear pair is in contact, vibrations occure. These vibrations are source of noise produced by revolving gears. Technical plastics were considered as a suitable

alternative material for gears. They have better damping and self-lubricationg properties than metallic materials. [27]

Use of technical plastic materils against metallic materials is at the expense of rigidity, strength and reability. Technical plastics is not recommended for gearing which has high revolutions or is transmitting high loads. Owning to slippage, heat is generated on teeth surfaces. Due to high values of angular velocity, low heat capacity of plastic material and lack of cooling, gears can easily heat up. This can lead to decrease of material strength and result in gear failure. Therefore, selection of suitable material for gears is essential. [28]

The most suitable materials for gear applications are:

- PA 6 (Polyamide 6): this material is wear resistant and absorbs impact even under rough conditions, but it is less suitable for small precision gears.
- PA 66 (Polyamide 66): compared to PA 6, this extruded polyamide offers better wear resistance (except against mating surfaces of high quality), absorbs less moisture and is dimensionally more stable, but it is also less suitable for small precision gears. 3) PA 6 G (Cast Polyamide 6): the high degree of crystallization makes PA 6 G especially wear resistant.
- Calaumid 612/612-FeÆ (cast PA 6/12): this polyamide is engineered toward toughness against shock loads, with wear resistance similar to PA 6 G. (Calaumid is a Timco exclusive)
- Calaumid 1200/1200-Fe (cast PA 12): a lower degree of moisture absorption gives better dimensional stability. It has excellent wear resistance and withstands high shock loads.
- PA 6 G + Oil (Cast Polyamide 6 + Oil): the addition of lubricating oil into the PA 6 G provides very good dry running and wear resistant properties.
- POM-C (Polyacetal-C): this Acetal absorbs very little moisture, which makes it suitable for precision gears, but it needs continuous lubrication under high loads.
- Polyetheretherketone (PEEK): excelent mechanical properties, very good mechanical strength and termal stability, high rigidity and wear resistence. Applications for gear whees, friction bearings, parts for automotive applications. Recommended for highly stressed parts. The polyetherentherketone semi-finished products can be produced in extrusion or moulding processes. [28]

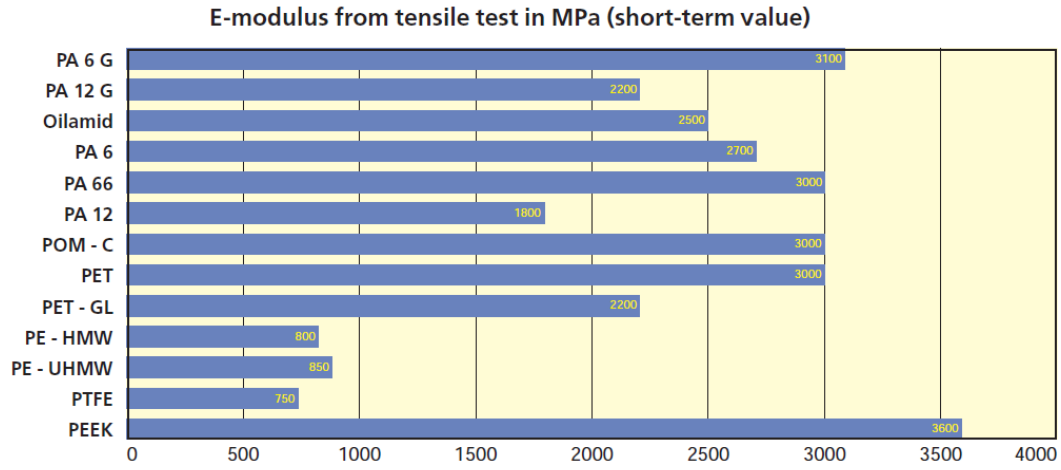

Fig. 3.51: Young's modulus comparation of selected engineering plastics [29]

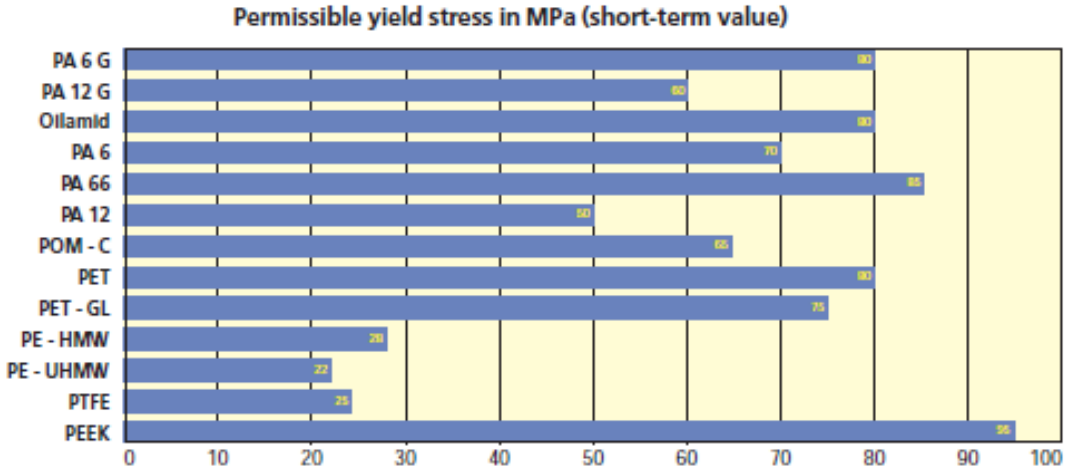

Fig. 3.52: Permissible yield stress comparation of selected engineering plastics [29]

From the mechanical value perspective PEEK is the most suitable material for geer wheels application. The biggest disadvantage is higher price of this material. An alternative material to polyetherentherketone is Polyamide 6 G, which has good mechanical properties. With respect to the results of following stress calculation it was decided to use modified polyetherketone (PEEK-GL).

Tab. 3.11: PEEK-GL material properties related to DIN 53 479 [29]

Parameter	Symbol	Value
Density	ρ_{PEEK}	1480kg/m^3
Yield Stress	σ_{PEEK}	118MPa
Modulus of elasticity resulting from tensile test	E_{PEEK}	8,1GPa

In the next step, it was necessary to verify the width of the gearing b_1 with respect to the chosen material properties. The maximal peripheral force F_u acting on pitch diameter is defined as:

The maximal peripheral force

$$F_U = \frac{2 \cdot M_1}{D_1} \tag{53}$$

$$F_U = \frac{2 \cdot 148{,}3}{0{,}048} = 6179{,}2N \tag{54}$$

Calculating the root strength of teeth

If the tooth root stress σ_F exceeds the permissible stress of the plastic pinion σ_{PEEK} under loading, it must be assumed that the teeth will break. For this reason the tooth root stress must be evaluated and compared with permissible value.

$$\sigma_F = \frac{F_U}{b_1 \cdot m} \cdot K_B \cdot Y_F \cdot Y_\beta \tag{55}$$

$$\sigma_F = \frac{6179{,}2}{40 \cdot 3} \cdot 1{,}12 \cdot 1{,}2 \cdot 1{,}0 = 69{,}20MPa \tag{56}$$

Where:
K_B…operating factor for different types of drive operation [29]
Y_F…tooth shape factor [29]
Y_β…helix factor to take account of the increases load bearing capacity in helical gearing, as this is the case with plastic spur gears, this value is to be set as 1,0 [29]

Safety factor

$$k_1 = \frac{\sigma_{PEEK}}{\sigma_F} \tag{57}$$

$$k_1 = \frac{118}{69{,}20} = 1{,}70 \tag{58}$$

The safety factor k_1 was evaluated against the limit of material elasticity. From perspective of variable load conditions value of safety factor is sufficient. Face width b_1 also satisfies dimension requirements given in table 8.

Other calculation methods could include thermal analysis of gear wheel body during loading conditions or define gear fatigue behavior. These situations can be solved analytically or by using of finite elements methods. In terms of this thesis, only the calculation of the stress in tooth root was realized.

3.7.4 PINION-SHAFT CONNECTION

Rounded-end (closed) key was used to transmit torque from an output shaft of rotary actuator to the pinion. This commonly used solution was choosen with respect to cost and manufacturing perspective. A key has two failure mechanisms which can be solved by numerical methods. The key can be sheared off and it can be crushed due to the compressive bearing forces. Calculation algorithm of key connection consists of two parts: shear stress analysis (equation 57) and bearing stress analysis (equation 61). The situation is illustrated in the figure below 3.53.

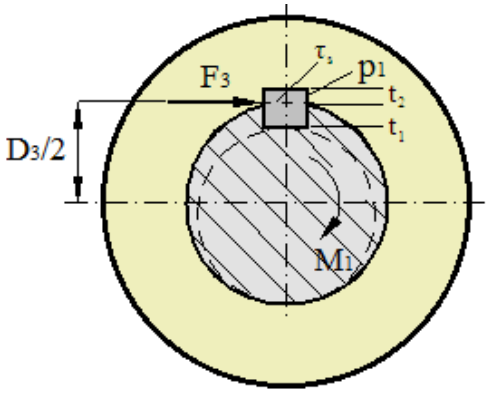

Fig. 3.53: Key connection with highlighted parameters

Force of shaft on key

$$F_3 = \frac{2 \cdot M_1}{D_3} \tag{59}$$

$$F_3 = \frac{2 \cdot 9{,}85}{0{,}0125} = 1576N \tag{60}$$

The serial version of the motor is supplied with a keyway in nominal key width b_2 = 5mm, nominal key length l_1 = 25mm. Permissible shear stress of modified polyetheretherketone (PEEK-GL) is 55,2MPa. [30]

Shear stress analysis

$$\tau_s = \frac{F_3}{S_1} = \frac{F_3}{l_1 \cdot b_2} \leq \tau_p \tag{61}$$

$$\tau_s = \frac{1576}{5 \cdot 25} = 12{,}6MPa \tag{62}$$

Safety factor

$$k_2 = \frac{\tau_d}{\tau_s} \tag{63}$$

$$k_2 = \frac{55{,}2}{12{,}6} = 4{,}38 \tag{64}$$

Safety coefitient of shear stress value is sufficient for door mechanism application.

Bearing stress analysis

Nominal keyway depth in shaft is eaquel to keyway depth in pinion t_1=t_2=2,5mm (parameters are illustrated in figure 3.53). A permissible compressive stress of modified polyetheretherketone (PEEK-GL) is p_p=138MPa. [30]

$$p_1 = \frac{F_3}{t_1 \cdot l_1} \leq p_p \tag{65}$$

$$p_1 = \frac{1576}{2{,}5 \cdot 25} = 25{,}21MPa \tag{66}$$

Safety factor

$$k_3 = \frac{p_p}{p_1} \tag{67}$$

$$k_3 = \frac{138}{25{,}21} = 5{,}47 \tag{68}$$

Safety coefitient of compress stress value k_3 has a sufficient value for door mechanism application. Axial securing of the pinion on shaft is realized by two locking rings.

3.7.5 CURVED GEAR RACK-DOOR CONNECTION

The connection between the door and the curved gear must be reliable, cheap and lightweight. These requirements indicate use of bolt connection. Torque transfer from curved gear rack to door structure is based on friction amongst two surfaces.

In this chapter, the calculation is focused on number and dimensions of used bolts which are required for torque transfer. The door structure is considered as hand laminated part. Therefore the use of inserts in door structure is needed.

The calculation is analyzed analytically in software *MathCAD*. Based on input parameters shown in table 3.12 two key values were estimated: safety coefficient related to elasticity limit of the bolt k_4 and pressure in threads p_t. Below there are listed only the most important parameters. The full calculation is attached in the appendix of thesis.

Tab. 3.12: Important parameters for curved gear rack – door connection

	Paramenter	Symbol	Value
Input parameters	Bolt size (M5)	D_b	5mm
	Bolt yield strength (class 6.6)	R_{e1}	480MPa
	Number of used bolts	n_b	4
	Pitch circle diameter	D_p	736mm
	Friction coeficient	f_1	0,4
	Maximal moment	M_1	148,3Nm
	Number of screwed threds inside each insetr	n_t	10
Results	Operational force from moment acting on one screw perpendicular to its axis	F_b	100,7N
	Safety coefficient related to elasticity limit of the bolt	k_4	8,2
	Pressure in threads	p_t	6,64MPa

High value of safety coefficient k_4 and low pressure in thread guarantee high reability of connection.

In software PTC Creo Parametric detailed 3D models of pinion and curved gear rack were created. These models can be edited by changing assigned parameters.

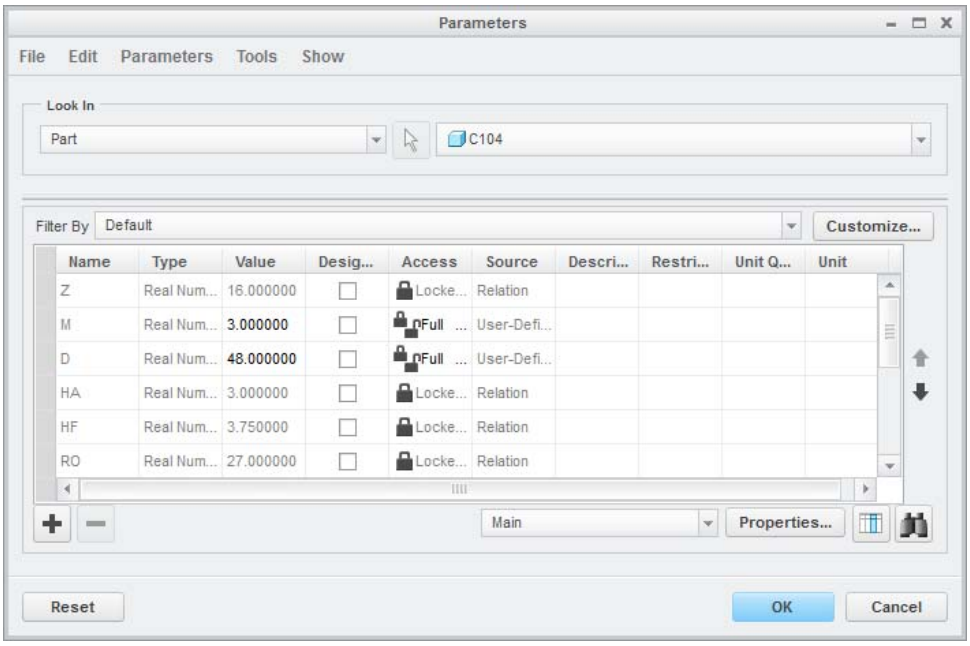

Fig. 3.54: Pinion parameters in PTC Creo Parametric environment

Fig. 3.55: Final 3D CAD models of gear curved rack and pinion (displayed with different scales)

3.7.6 LINEAR RAIL PROPOSAL

A force analysis was required to select an appropriate linear rail system. The situation is solved as statically determinate model in the maximal extended rail position.The selection of suitable rail system is primarily limited by moments M_x, M_y, M_z (shown in figure 3.56). The load condition is considered as the course of the door opening when aerodynamic force is applied, together with the inclusion of the gravitational force and the maximum force developed by rotary actuator.

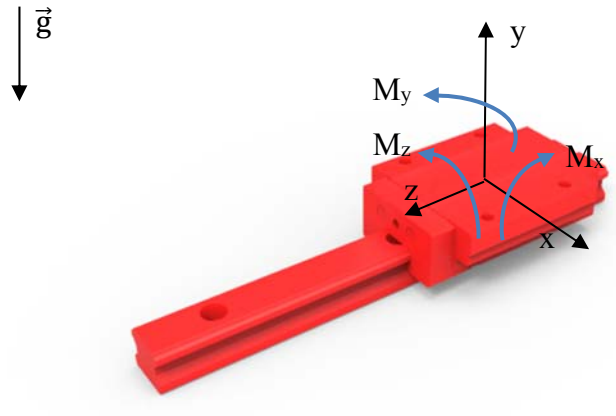

Fig. 3.56: Linear rail with displayed force and Cartesian coordinate system

Figure 3.57 illustrates forces applied on system in *yz* plain. This situation represents the position of the maximum opened door when applying aerodynamic pressure and gravitional force. The maximum value of the moment M_{XLIN} is determined by two force vectors. Vector F_{A1} represents the highest magnitude of the aerodynamic force caused by velocity of fluid applied on open door in point *1* (center of pressure of surface S_1), meanwhile door weight acts in point 2 (center of gravity). Both points have a certain position in the Cartesian coordinate system defined by parameters d_2 and d_6 shown below.

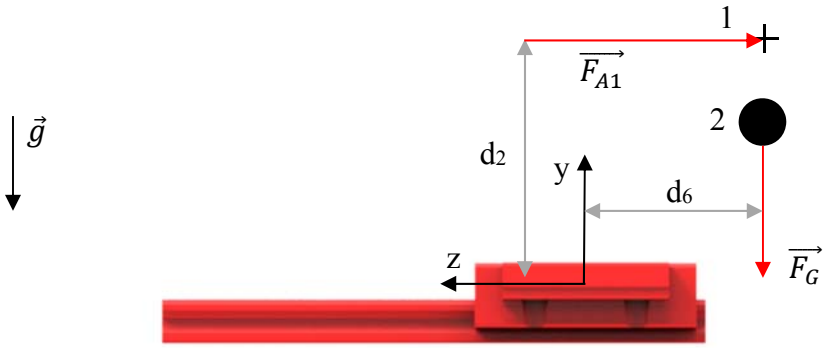

Fig. 3.57: Linear rail with displayed forces in yz plain

$$\sum M_x = 0 \tag{69}$$

$$M_{XLIN} = F_{A1} \cdot d_2 + m_1 \cdot g \cdot d_6 \tag{70}$$

$$M_{XLIN} = 163 \cdot 0{,}782 + 16{,}03 \cdot 9{,}81 \cdot 0{,}18 = 155{,}7Nm \tag{71}$$

In plane xz the door in closed position is described. The force vector F_{A2} acts on center of pressure (point 1). The maximum magnitude of force F_u is in the beginning of the door opening process.

$$\sum M_y = 0 \tag{72}$$

$$M_{YLIN} = F_{A2} \cdot d_4 + F_U \cdot d_7 \tag{73}$$

$$M_{YLIN} = 260 \cdot 0{,}609 + 6179{,}2 \cdot 0{,}064 = 553{,}8Nm \tag{74}$$

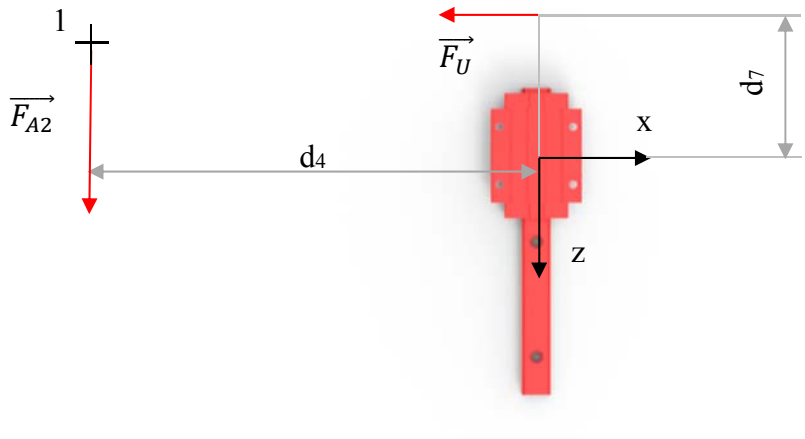

Fig. 3.58: Linear rail with displayed forces in xz plain

The maximum moment in the z axis was already expressed in the chapter 3.6.1.

$$M_{ZLIN} = M_1 = 148{,}3Nm \tag{75}$$

Based on market analysis linear recirculating ball guide from company HepocoMotion was choosen. The HLG range offers smooth low friction movement, high rigidity and an excellent load capacity. The unique bleed lubrication system that enables block to be re-greased through the rail, making it easy to set up an automatic lubrication facility. The product HLG 25RL has compact dimensions and fulfils load parameters. [31]

Tab. 3.13: Maximal observed values compared to load capacity of selected linear rail [31]

Parameter	Symbol	Maximal observed operating load	HLG 25RL load capacity
moment in x axis	M_{XLIN}	155,7 Nm	596Nm
moment in y axis	M_{YLIN}	553,8 Nm	596Nm
moment in z axis	M_{ZLIN}	148,3 Nm	525Nm

Tab. 3.14: Parameters of selected linear rail system HLG 25RL [31]

Parameter	Value
HLG rail weight	3kg/m
HLG block weight	0,71kg
Operation temperature	-35°C to +80°C
Rail material	stainless steel

Fig. 3.59: CAD model of the HLG25RL linear rail system

3.7.7 CURVED RAIL DESIGN

For control of object motion along curved trajectory, the use of the curved line system is an ideal choise. Curved rail systems are often used for automotion applications where an accurate motion control and rigid system are required. On the market there exist normalized curviline sliders and rails for constant or variable trajectory radius. For application in vehicle Uniti is constant rail required.

General rail characteristics:

- maximum slider operating velocity on the rail: 1.5m/s,
- maximum acceleration: 2m/s^2,
- temperature range from -30 °C to +80 °C,
- rails and runner electrolytic zinc-plated and passivated. [32]

To select a suitable rail system type, it is necessary to determine load conditions applied on components. The main load components include the raxial and axial forces acting on the body of the slider.

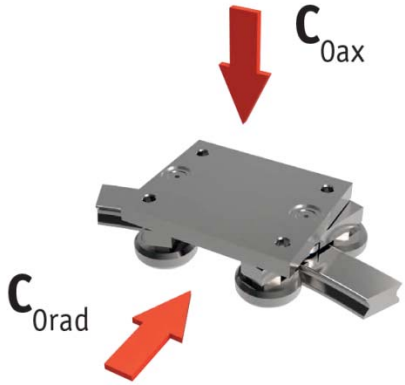

Fig. 3.60: Primary load capacities of curved line rail system [32]

The calculation of the loads applied on the body of the slider is divided into two situations. The first situation determines radial load applied on the slider during door movement. In this case, the centripetal force F_{SC} and component of gravitational force F_{GA} act on slider (note: radial component of gravitional force F_{GR} is captured by force F_U applied on the diametral pitch of the pinion). The friction between rail and sliders is neglected.

The first situation is illustrated in figure 3.61. Point 1 represents the body of the slider. Point 2 shows position of center of gravity of door. The distance between trajectory of CoG and curved rail is d_8. The magnitude of centripetal force depends on angular velocity during door opening or closing process and door weight.

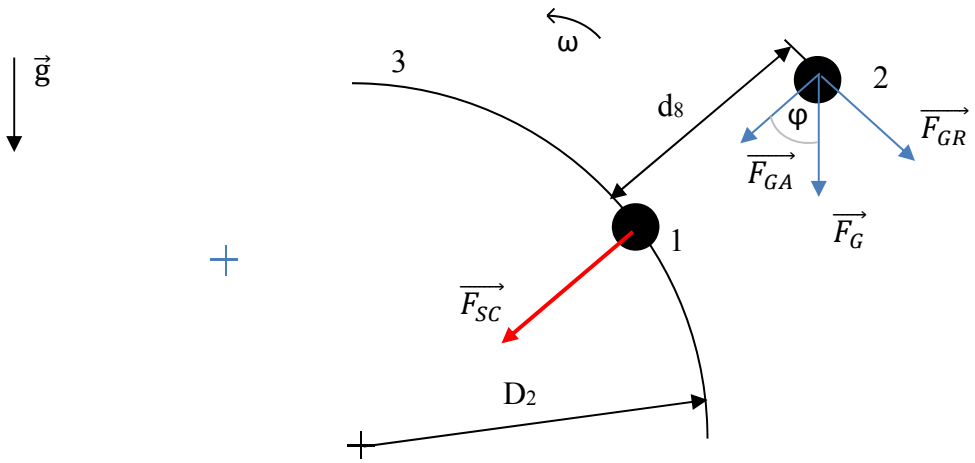

Fig. 3.61: Depicting of forces acting on the slider

Data observed in the kinematic analysis chapter 3.5 was used to calculate the centripental force in following equations.

Centripetal force:

$$F_{SC} = m_1 \cdot (D_2 + d_8) \cdot {\omega_{MAX}}^2 \tag{76}$$

$$F_{SC} = 16{,}03 \cdot (0{,}72 + 0{,}148) \cdot 0{,}76^2 = 8{,}03N \tag{77}$$

Axial component of gravitational force:

$$F_{GA} = m_1 \cdot g \cdot \sin(\varphi_2) \tag{78}$$

$$F_{GA} = 16{,}03 \cdot 9{,}81 \cdot \sin(60) = 136{,}2N \tag{79}$$

From the detected value of the centripetal force arises, that the magnitude of axial component of gravitational force is much higher. The maximum value of axial component of gravitational force is in opened door position φ_2. This value is considered as maximum radial load applied on slider.

The maximum value of axial force applied on slider is considered as aerodynamic force F_{A2} which was observed in the chapter 0.

Based on detected values product *Curviline* developed by manufacturing Rollon® was selected. The number of the selected product is GCT01-180-45. This product disposes sufficient load capacity, rigidity and movement accuracy.

Tab. 3.15: Comparation of operating load and load capacity of the curviline GCT01-180-45[32]

Parameter	Maximal operating load	GCT01-180-45 load capacity
Radial force	136,2N	1110N
Axial force	260N	1600N

Tab. 3.16: Properties of selected rail system GCT01-180-45 [32]

Parameter	Value
Rail weight	1,1kg/m
Slider weight	0,4kg
Operation temperature	-30°C to +100°C
Material	stainless steel

Fig. 3.62: CAD model od the product Curviline GCT01-180-45

3.7.8 ACTUATOR HOUSING DESIGN

The actuator housing is an important part which connects most of the components of the system together. Housing must be designed with respect to all loading conditions. At the same time, it must meet requirements for low weight, manufacturing process and cost.

From the initial component layout in the concept section 3.4.4, a design based on profiled 5mm sheet metal was created. The linear rail, linear actuator, rotary actuator and two roller guides are connected to the housing. From the manufacturing perspective it is a component design based on laser cutting, bending and welding technology process. The actuator housing consists of five parts welded together. All parts are illustrated in figure 3.63.

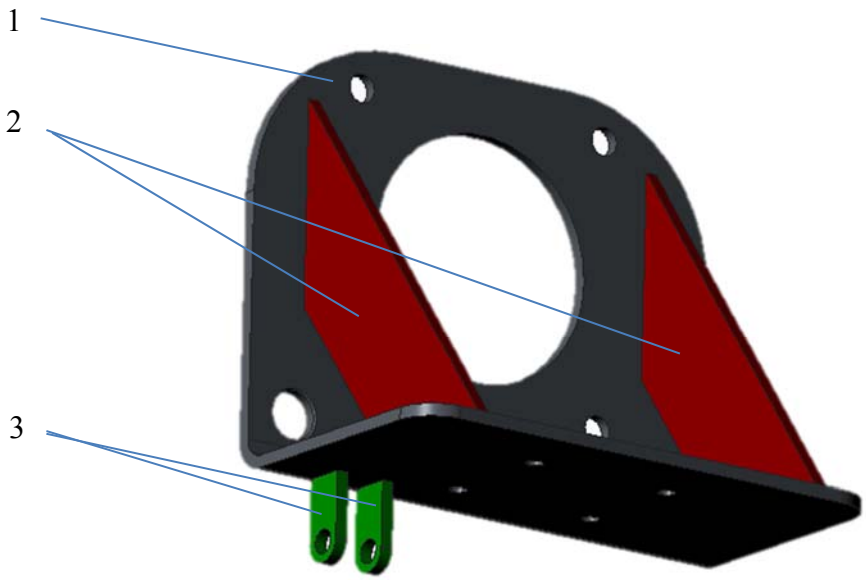

Fig. 3.63: The actuator housing design, 1 – actuator body, 2 – supporting rib, 3 – attachment point for linear actuator

Connection dimensions of all components to the actuator were essential input parameters for component design. Ribs are chosen to increase stiffness of part. Linear actuator is connected to the housing by four M6 screws. Two holes in actuator housing body substituted the *Curviline* guide body (rectangular structure visible in figure 3.62). This design modification led to a weight reduction of 210 g. The rotary actuator is connected to the housing by four M6 screws.

After the verification process of proposed packeting and collisions in the assembly, the actuator housing was subjected to a static structural stress analysis within software PTC Creo Simulate. In the first step of stress analysis, material properties (values of Young's modulus, poisson constant, both for steel) were verified. In the next step there were applied loads, which represent situation of applied full moment: 148Nm developed by rotary actuator.

Based on moment equilibrium there were observed forces reactions in rotary housing attachment points. The detected forces from following equations are used as input parameters for analysis.

$$\sum M_Z = 0 \tag{80}$$

$$F_R = F_{R1} = F_{R2} = F_{R3} = F_{R4} \tag{81}$$

$$M_Z = 4F_R \cdot d_7 \tag{82}$$

$$F_R = \frac{M_Z}{4d_7} \tag{83}$$

$$F_R = \frac{148}{4 \cdot 0{,}05} = 740N \tag{84}$$

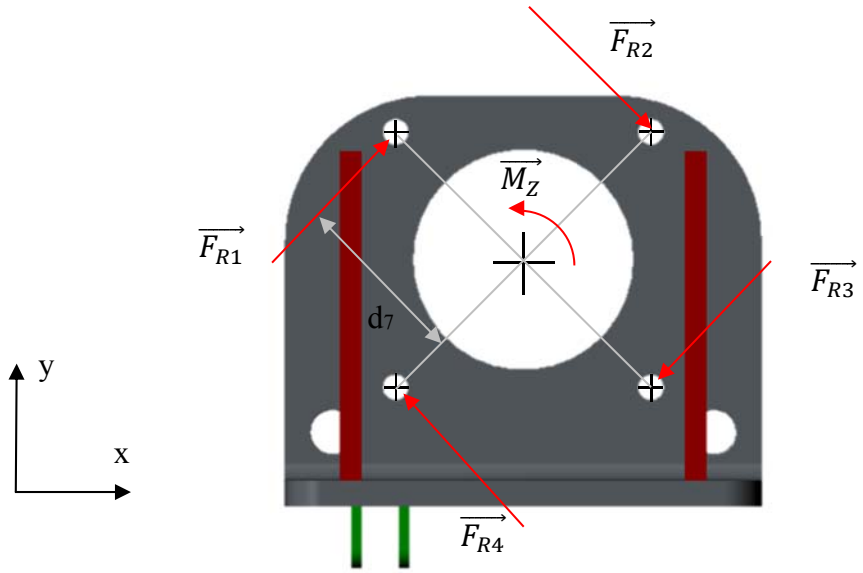

Fig. 3.64: Forces reactions and dimension shown on actuator housing in plain xy

According to Pythagorean theorem, the magnitude of the force was spread over two axes. Then, the vectors of forces with respect to the coordinate system are given:

$$\overrightarrow{F_{R1}} = (523\vec{\imath} + 523\vec{\jmath})N$$

$$\overrightarrow{F_{R2}} = (523\vec{\imath} - 523\vec{\jmath})N$$

$$\overrightarrow{F_{R3}} = (-523\vec{\imath} - 523\vec{\jmath})N$$

$$\overrightarrow{F_{R4}} = (-523\vec{\imath} + 523\vec{\jmath})N$$

The circumferential force F_U acting at the contact point of the two gears (tangential to the diametral pitch D_1) at distance d_7 (from the center of attachment point between actuator housing and rail), causes moment M_y in y axis. Forces reactions acting in actuator mounting holes are named as: F_{R5}, F_{R6}, F_{R7}, F_{R8}. These forces reactions act on the arm d_8. With respect to moment equilibrium there were calculated force vectors:

$$\sum M_Y = 0 \tag{85}$$

$$F_U \cdot d_7 = (F_{R5} + F_{R6} + F_{R7} + F_{R8}) \cdot u = F_{XR} \cdot d_8 \tag{86}$$

$$F_{XR} = \frac{F_U \cdot d_7}{d_8} \tag{87}$$

$$F_{XR} = \frac{6179{,}2 \cdot 0{,}064}{0{,}038} = 10\,407N \tag{88}$$

$$F_{XR} = F_{R5} + F_{R6} + F_{R7} + F_{R8} \tag{89}$$

$$F_{R5} = \frac{F_{XR}}{4} = \frac{10\,407}{4} = 2601N \tag{90}$$

$$\overrightarrow{F_{R5}} = \overrightarrow{F_{R6}} = \overrightarrow{F_{R7}} = \overrightarrow{F_{R8}} = (2601\vec{\imath})\ N \tag{91}$$

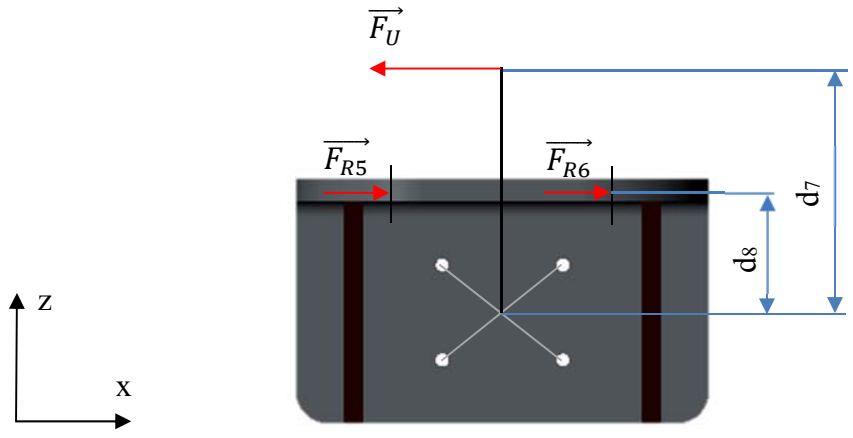

Fig. 3.65: Forces reactions and dimension shown on actuator housing in plain xz

The moment caused by gravitational force component was due to its low value neglected. Force vectors were applied on actuator by components. Four fixed supports applied on holes represents the connection between actuator housing and linear rail. The fixed support constraint restricts displacement in x,y,z directions.

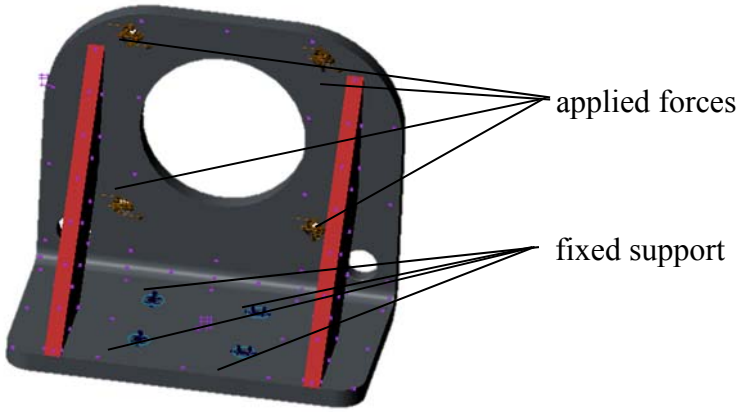

Fig. 3.66: Loads and contstrains applied on actuator housing

In the next step, a computational mesh was generated. Tetrahedron type elements were selected. The size of the body filling elements was 4 mm. At the screw attachment, an auxiliary volume was created, in which the computational network was filled with a 1mm element. This mesh adjustment leads to more precise results in area of the screw holes. The total number of elements was 8610.

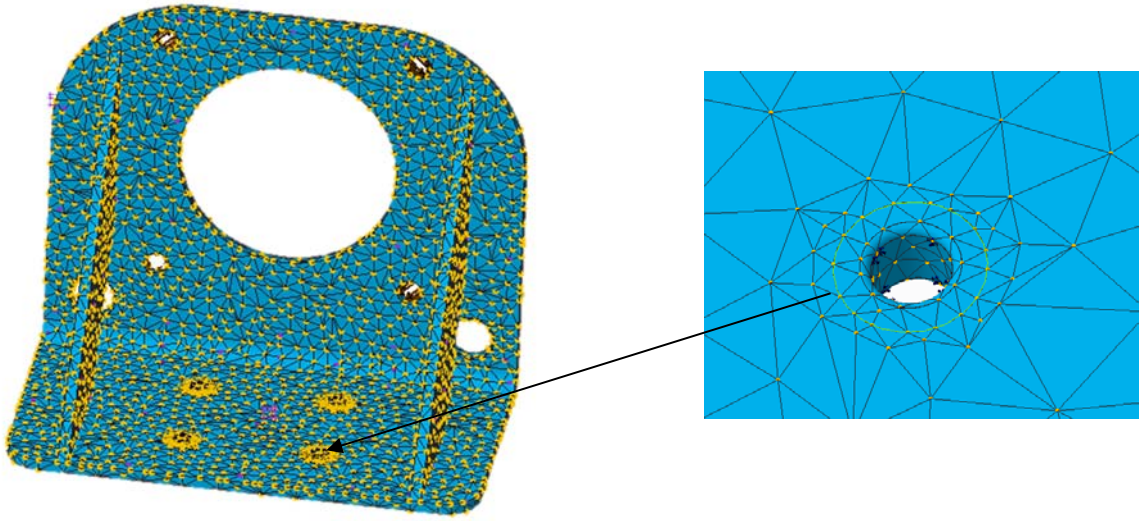

Fig. 3.67 Meshing process (left – actuator housing, right – detail on mesh adjustment around a hole)

After completing the analysis, results were interpreted by using of magnitude displacement and von Mises stress.

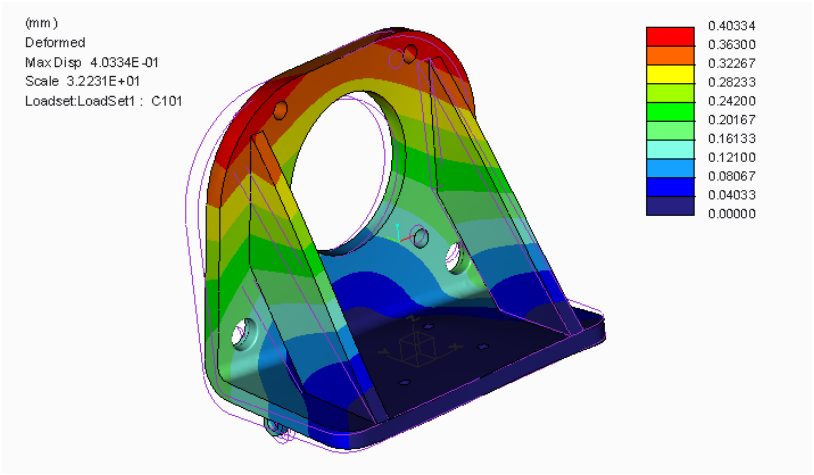

Fig. 3.68: Total deformation of actuator housing

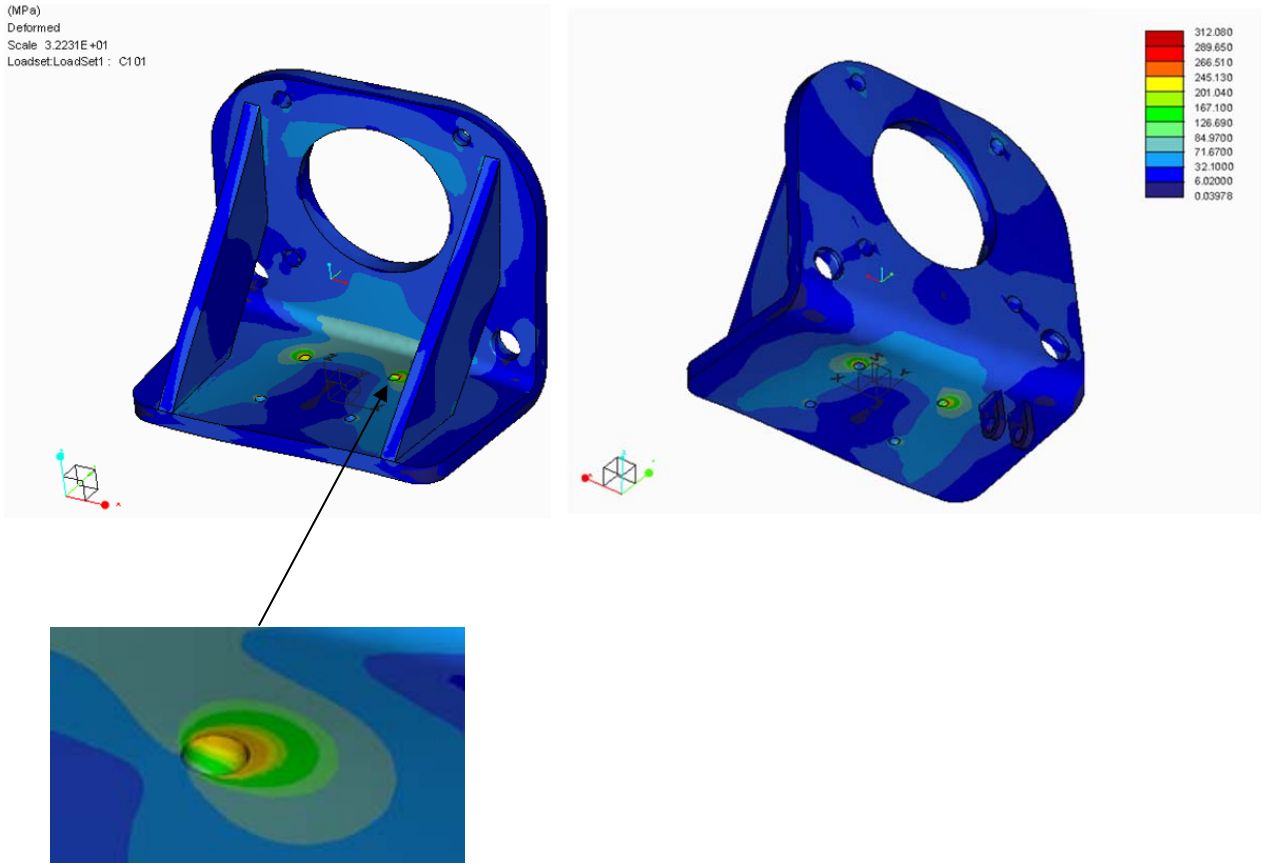

Fig. 3.69: Results from stress analysis (equivalent - von Mises stress is illustrated)

The maximum value of von Mises stress was achieved 312MPa (shown in figure 3.69). However this stress peak occurred in attachment point in very little area where fixed support was applied. More relevant value of 272MPa was considered as possible maximum value.

Tab. 3.17: Results from static structural analysis of actuator housing

Parameter	Symbol	Value
Maximum equivalent stress (von Mises)	σ_{RED}	272MPa
Maximum total displacement	δ	0,40mm

Due to the achieved values of maximum von Mises stress and total displacement, the use of steel is appropriate for the current design. As shown in the figure 3.69, it is possible to achieve lower mass of the actuator housing by shape optimization. For use in serial production, all load conditions, including fatigue analysis, must be considered.

3.7.9 SAFETY ITEMS

The main task of safety items is to prevent injuries. Malfunctions related to door movement can be dangerous for passangers and have a negative impact on manufacturing brand and its products. Therefore, it is necessary to bring to the market safe products that will always fulfill their function in given conditions and with proper use of the product.

Fig. 3.70: Wing door system implemented on Tesla Model X [33]

One example of the door opening system error is the crossover Tesla Model X. Tesla's falcon wing door system has poor detection of obstacles, or conversely does not want to close – this problem was named as "a ghost obstruction". Tesla model X is equipped with capacity and pinch sensors. [34] The system has a problem with obstacle detection primarily at the top of the body because of the absence of sensors. The mechanism can develop high forces that can injure the passenger. In response to this issue, many user reviews have been published to highlight this problem. Tesla has partially solved this problem by updating the firmware.

Fig. 3.71: Example of user's review: [retrieved from video source: http://bit.ly/2rIylcK]

Electrical sensing edges

Electrical sensing edges are used for protecting crushing and shearing points on automatic doors, gates and grids. Rubber profiles of different sizes in combination with various switching devices protect people and objects safely and reliably according to the applicable standards. [35] They are based on the tried-and-tested principle of the drawing the contact strip into the rubber profile. Even with only minimal pressure, the conductive rubber profiles are pressed against one another and the opening pulse is forwarded to a switching device or a transmission system. The technical design ensures high reliability even in unusual applications.

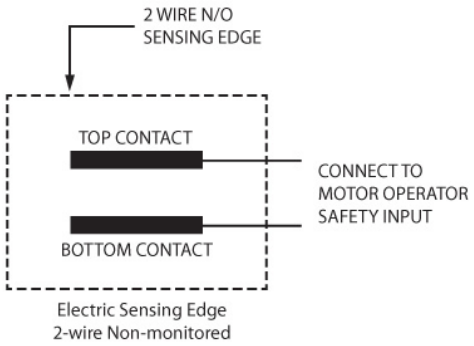

Fig. 3.72: Principle of sensing edges [36]

The figure 3.72 shows a basic 2-conductor electrical configuration. The outer covering houses 2 electrically conductive flexible contact elements. When touched, the edge compresses causing the contacts to touch. An immediate electrical signal is sent to the motor control unit to stop and/or reverse motion.

There are several versions of these pinch sensors on the market. They are mainly used for industrial applications. Most sensors are not suitable for application in Uniti vehicle due to its large dimensions. Within the further development process, a low profile door seal with electrical sensing edges principle would be achived.

Fig. 3.73: Demonstration of pinch sensor function used for Tesla wing door system [retrieved from video source: http://bit.ly/2rIylcK]

Position encoder

Another way to prevent user injuries is to use an electro-mechanical device that converts the angular position to the code - the rotary encoder. This device is already implemented in a selected brushless servomotor. By comparing the data between the current position and the door opening process, environmental resistance can be detected. This method must include a deviation from the ideal course in order to take into account the environmental resistance and thus avoid spontaneous stopping of the door opening and closing processes. In case of the deviation from the ideal characteristics, central processing unit emits signal to actuator which will stop the door movement. The size of tolerance field for door position characteristic can be evaluated during prototype development process.

Capacitive sensors

Nowadays capacitive sensors expands trought different applications. *„ In capacitive touch sensors, the electrode represents one of the plates of the capacitor. The second plate is represented by two objects: one is the environment of the sensor electrode which forms parasitic capacitor C_0 and the other is a conductive object like human body which forms touch capacitor C_T. The sensor electrode is connected to a measurement circuit and the capacitance is measured periodically. The output capacitance will increase if a conductive object touches or approaches the sensor electrode. The measurement circuit will detect the change in the capacitance and converts it into a trigger signal.“[37]* The principle of a capacitive touch sensor is shown in bellow figure*:*

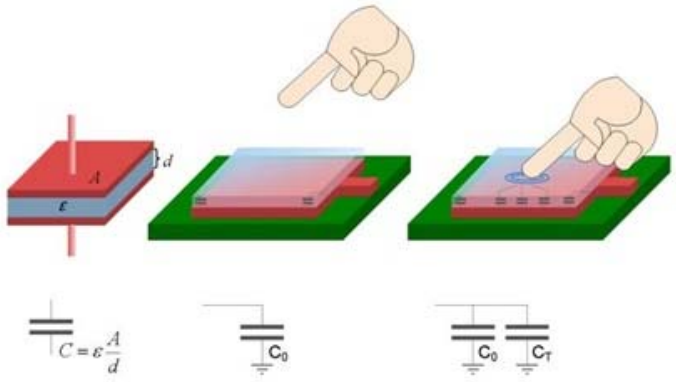

Fig. 3.74: Principle of contact capacitive sensors [37]

Fig. 3.75: Capacitive type sensor applied on outer Tesla wing door (matte black) surface [retrieved from video source: http://bit.ly/2rIylcK]

By using a combination of sensors mentioned above it is possible to ensure high safety of door mechanism system. The contact capacitive sensors can be applied on two door surfaces illustrated in figure 3.74. Pinch sensors can be deploymented on door edges. The selection of particular sensor type is above the scope of this thesis.

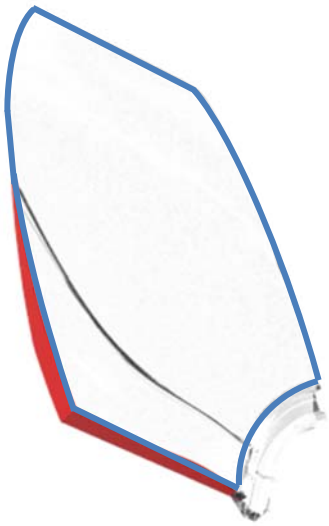

Fig. 3.76: Sensors applied on door (red color - capacitive type; blue color - pinch sensor type)

3.7.10 COMPONENT MODIFICATIONS

In order to meet functionality of proposed system, it was necessary to modify some components. The most noticeable modification is related to door design. It was necessary to create a ceating faces for curved gear rack and curved rail.

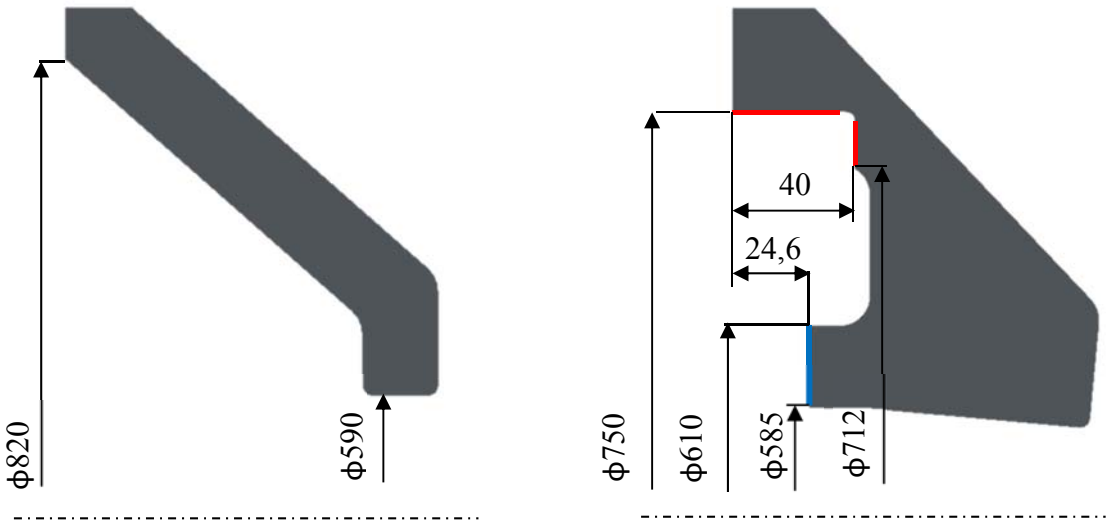

Fig. 3.77: Left side: old door cross section, right side: modified door cross section with highlighted dimensions [mm], red colored lines are contact surfaces for curved gear rack, blue line is contact surface for curved rail

The next modification concerns the rotor of the linear actuator. The standard rotor needs to adjust one end for connecting the end rod that is connected to the actuator housing. Therefore

it is recommended to make inner thread M5 inside the linear rotor body and adjust rotor shape for a wrench 10 mm. The total length of the serial rotor must be extended to 180mm.

Fig. 3.78: Modified CAD model of linear rotor

The rotary output shaft of the actuator must be extended due to the pinion width. The key dimensions have been retained. New locking ring grooves appear on the output shaft due to axial pinion protection on the shaft. This change will require negotiations with the engine supplier.

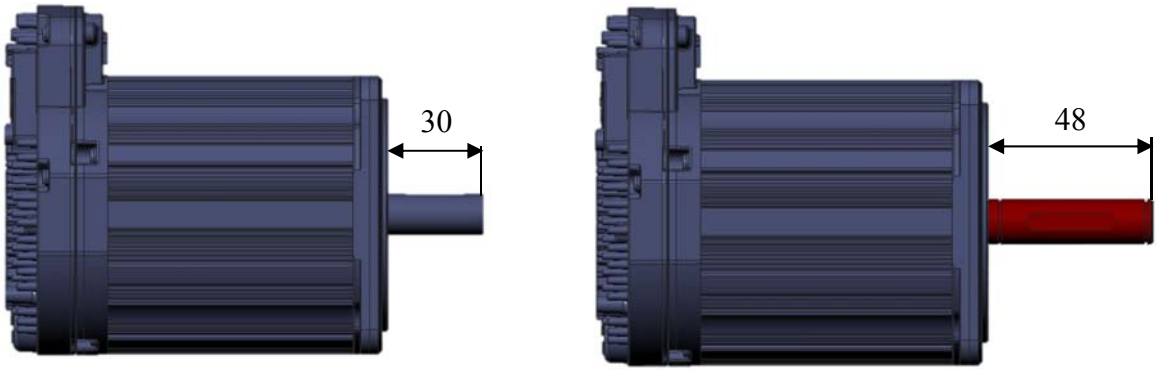

Fig. 3.79: Rotary actuator modification with highlighted dimensions [mm]

At the ends of the linear guide and the curved rail it is recommended to drill a hole for the mechanical stops.

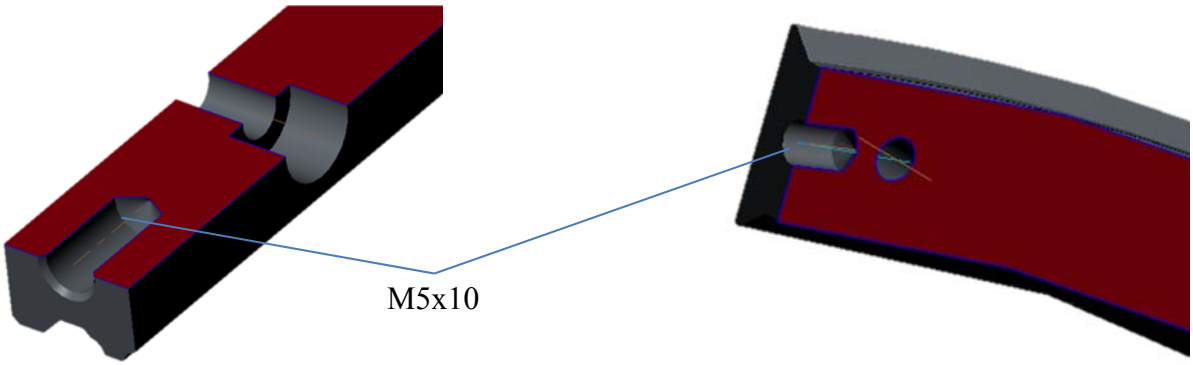

Fig. 3.80: Drilled holes for mechanical stops M5 in linear rail (left side), and in curved rail (right side)

3.8 SYSTEM CONTROL

This chapter summarizes the description of each door system step during its operation conditions. Mentioned door locks have not been designed yet. However, in this chapter they are included to describe sequence of door mechanism system processes.

When the door is opening, system locks (lock 1 and lock 2) are deactivated, which limits the movement of the door while driving. After deactivation of the safety locks function, the linear actuator is activated. The linear actuator ejects door according to the speed characteristic shown in Fig. 3.32. When the linear movement is complete, a linear safety lock (lock 2) restricting the movement of the mechanism along linear rail is activated. The element that confirms the end position of the ejection is the contact switch.

Then lock 3 is deactivated and the rotary actuator is running according to the speed characteristic shown in Fig. 3.33. The element that confirms the end position of the ejection is the contact switch. At this moment, it is important to fix the door position. Therefore the third safety lock 3 is activated. After locking the door position by two safety locks, passangers can safely enter or egress the vehicle.

To close the door, it is necessary to deactivate the door lock 3 which fixes rotation of door mechanism. A rotary actuator can develop moment accorging to door closing characteristic. The end position is again verified by the contact switch. Once the desired door position is reached, a safety lock limiting the linear movement along linear rail is deactivated. The linear actuator can develop force to close the door. At the end of the linear motion, the end position is verified by the contact sensor. The last phase involves the activation of the door locks.

If the conact between the door and some obstacle will be recognised, the opening or closing process will be stopped immediately. The design of door locks is important also for reinforcing the door structure during a car accident. After summarizing the procedure, it is evident that two contact sensors and three security locks have to be implemented.

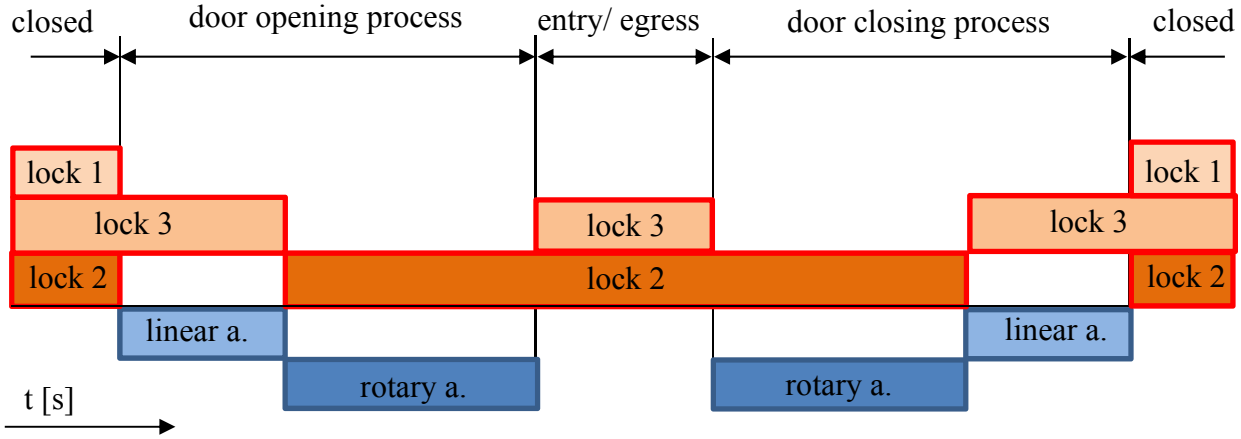

Fig. 3.81: Description of safety locks and actuators sequences in time domain

4 DISCUSSION

Total door opening or closing time can be reduced by overlapping translation and rotation door movement. In this new situation, a dynamic analysis must be carried out again and the design of the parts must be checked.

Door properties (weight, position of centre of gravity, moments of inertia) and door motion characteristics have a direct impact on actuator selection. By reduction of door weight or increasing the time of the door movement, lower load values can be achieved.

The calculation of the aerodynamic force is idealized and it is recommended to perform an adequate computational fluid dynamic analysis with more accurate quantification of load during selected weather conditions.

The linear actuator meets the performance requirements and compact size of the stator. The length of the rotor, however, can cause problems because it exceeds preliminary chassis boundaries in the initial door position by 42mm. An alternative solution to linear actuator can be another, smaller, rotary actuator which will propel gear rack mounted on actuator housing. Hereby door mechanism linear movement can be controlled by compact rotary actuator. A disadvantage of this alternative solution is complex construction which consists of another gear rack.

Helical gear design can reduce width of pinion and curved gear rack. From the manufacturing perspective a helical gear design is more complex than manufacturing process of spur gears. By using of helical gear pair there will arise axial force that acts on the rotor bearings.

The curved gear rack is designed from a premium technical plastic material – modified polyetheretherketone (PEEK). Injection molding can be considered only for mass production due to high price of molds and material. From the technological point of view, the precision of gear geometry must be taken into account. Additional machining may be required. The technological process must be consulted. If the use of the peek material for curved gear rack will be inappropriate, a metal material can substitute PEEK. This would result in smaller gear width but much higher weight.

The actuator housing is designed as weldment made from steel bended sheet metal. Its design can be relieved by futher stress analysis.

For further development of the bodywork, it will be crutial to design appropriate inserts for connection to linear rail.

The design of door locks plays an important role in general safety of door mechanism and its functionality. The System Management chapter shows a sequence of system features. Within prototype testing it is important to properly solve the transitions between involvement/ disconnecting operations of actuators and safety door locks.

From a safety point of view, it is necessary to allow egress from the vehicle when the vehicle is not moving. As part of the FMEA analysis, it is possible to identify possible problems and suggest ways how to prevent or avoid them. Together with the software department, it is important to manage the safety door locks correctly. After their deactivation, the door mechanism can manually opened.

Fig. 4.1: Iso views on CAD assembly of door mechanism system

CONCLUSIONS

Subsequently, three door concepts were described and analyzed. With regard to user requirements, concept 3 was chosen. The advantage of this concept is the ability to control the movement according to user requirements and acceptable dimensions.

For the chosen concept, a knematic analysis was developed accorting to selected velocity characteristics which meets user requirements. Afterwards results from the kinematic analysis were used as an input to dynamic analysis. Within dynamic analysis the load applied on mechanism was investigated. The maximum moment during door motion is 148Nm. Environmental resistance (aerodynamic force) during door mechanism operation has been taken into account. The maximum aerodynamic force F_{A2} acting in CoP (during opened doors) is 260N. The maximum forces observed from dynamic analysis were used for component design.

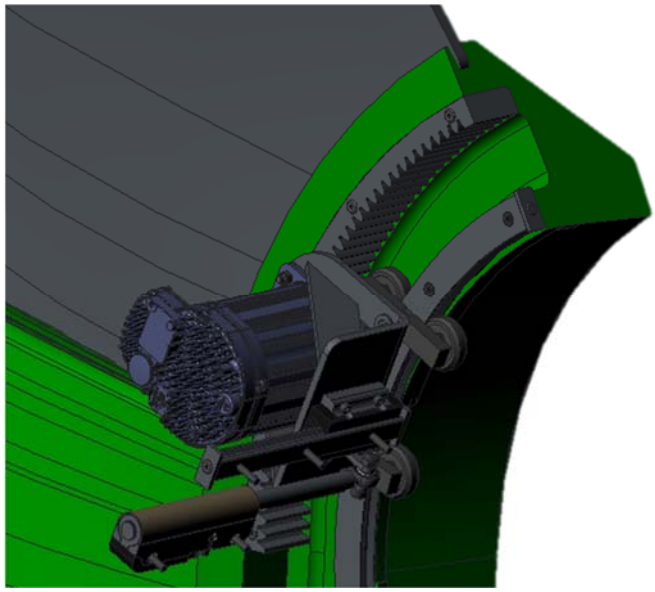

Fig. 5.0.1: Final assembly of door mechanism

Linear actuator selection is based on the requirements specified in the Dynamic Analysis chapter. Selected DC stator PS01-37Sx120F-HP-N-AGI meets performance characteristics and it has compact dimensions.

With regard to demanded performance and user requirements, a brushless DC servomotor CPM-SDHP-3432S-ELN has been selected. Chosen servomotor provides high performance, low noise emissions, and possibility to control its movement.

Afterwards, the gear ratio between rotary actuator and door was selected. The value of the selected gear ratio is 15. With this value, it was possible to verify the maximum speed of the servomotor. The maxium servomotor speed will not be reached during operating conditions.

The geometry of spur gear was designed in relation to dimensional possibilities in assembly and selected gear ratio. The geometric parameters of pinion and curved gear rack have been calculated. Results are presented in table 3.12. Within the analytical calculation, the value of stress in root of gear teeth was detected. For selected material, modified polyetheretherketone

(PEEK), the safety factor related to Yield strenght is 1,70. However, the gear width is 40 mm. Fatigue behavior was not observed in this thesis. It is reccomanded to observe cyclic loading in real prototype due to simulation complexity.

The next step was focused on verification of the connection between the output of servomotor shaft and pinion. The keyed joint was selected for torque transmission. A key has two failure mechanisms which where examinated. Calculated values of shear stress and bearing pressure meet permissible limits.

The connection between the door and the curved gear rack is realized by a screw connection. Based on the calculation, the number and size of the bolts were expressed in terms of safe moment transfer. It was decided to use 4 bolts with size M5. Safety coefficient related to elasticity limit of bolt is 8,2 and pressure in threads meets permissible limits.The complete calculation is attached in the appendix.

Subsequently, the moments applied to the linear rail system were expressed. Based on these values type HLG 25RL was selected. The curved rail proposal has taken into account axial and radial forces. Compared to the load-bearing capacity of the chosen type, the construction is suitable for application in Uniti vehicle.

Actuator housing connects most of the parts from door mechanism system. It transfers the load between the linear rail system and servomotor. Connection dimensions of components to the actuator were essential input parameters for its design. Finite element method was chosen to optimize the dimensions. As load case was choosen the maximum moment produced by servomotor during its operation. With respect to moment equilibrium, force reactions were determined. The vectors of these forces were inserted into the analysis. After geberating the computing mesh and running the analysis, the results of von Mises stress and total deformation were displayed. The maximum value of von Mises stress is 272 MPa. Maximum magnitude of total deformation is 0,40mm. Due to stress distribution, there is space for further optimization. However, it is necessary to take into account even more load cases and consider fatigue behaviour which was not part of this thesis.

Within the scope of further assembly modifications, the major component dimensions are based on parameters that can be modified. To achieve the door mechanism assembly, it was necessary to adjust some component design. All modifications are described in the chapter Component modifications.

To meet security requirements, the chapter Safety items presents three exaples of detection of obstacles during door motion. The system management chapter provides auxiliary view of processes of locks and actuators performed within the door movement.

The result of the work is a new concept of automatic vertical door opening mechanism. Weights of the components are shown in table 5.1. Due to the mass limit (450 kilograms) for light quadricycle category EU L7e, it will depend on the weight of other vehicle peripherals. If the total vehicle mass exceeds the limit, an alternative door mechanism must be also considered.

Tab. 5.1: Weight of the components

Component name	Weight [g]
Rotary actuator assembly	2810
Linear actuator assembly	941
Actuator housing	642
Linear rail	498
Linear rail guide	710
Curved rail	753
Curved rail guides	486
Curved rack	343
Pinion	90
Total assembly weight	7273

Costs of key system elements are shown in the table 5.2. The door mechanism cost can greatly influence OEM volume discounts. While Uniti is a premium class vehicle, the price has to be reduced to ensure competitiveness.

Tab. 5.2: Cost of selected components for volume (100-500 pieces)

Component	Supplier	Type	Price
Rotary actuator	Teknic	CPM-SDHP-3432S-ELN	$538
Linear actuator stator	LinMot	PS01-37Sx120F-HP-N-AGI	$116
Curved rail system	Rollon	GCT01-180-45	$56,9
Linear rail system	HepocoMotion	HLG 25RL	$86,1

Designed automatic door mechanism can at first sight engage the customer's attention with its unconventional movement. Nevertheless, from the construction perspective it is a complex and costly system which consists of sophisticated software management of the door movement with respect to safety requirements. Reliability of the system depends on several components, and it is necessary to develop a detailed design FMEA analysis in terms of safety and function and provide testing of the prototype on the test bench before it will be implemented to the vehicle. Unlike conventional door hinges, this door mechanism has a significant impact on the chassis and door design.

REFERENCES

[1] Technical specification. Uniti Sweden [online]. Lund, 2016 [cit. 2016-12-05]. Retrieved from: http://www.unitisweden.com/techspecs/

[2] Uniti with open door. Prlog.org [online]. 2016 [cit. 2016-11-03]. Retrieved from: https://www.prlog.org/12592707-uniti-with-open-doors.jpg

[3] Lamborghini patent. Patent images: Storage [online]. [cit. 2017-05-18]. Retrieved from: http://patentimages.storage.googleapis.com/US6808223B1/US06808223-20041026-D00000.png

[4] Lamborghini Aventador. Amazonaws [online]. 2016 [cit. 2016-12-05]. Retrieved from: https://s3.amazonaws.com/cn-static/si/sw1280/7606/7606_st1280_037.jpg

[5] Koenigsegg Agera: Geneva show. Johny Wheels [online]. [cit. 2017-05-18]. Retrieved from: http://cdn.johnywheels.com/2016/01/01/koenigseggagerardoors-l-d30e14845e451b99.jpg

[6] Door mechnism Koenigsegg Agera. WP Engine [online]. [cit. 2017-05-18]. Retrieved from: http://1hosj01irnixn8onr1zmv5s1.wpengine.netdna-cdn.com/wp-content/uploads/2015/12/Station2-29-of-81.jpg

[7] Alfa Romeo Pandion. US Technology World [online]. [cit. 2017-05-18]. Retrieved from: http://us.technogelworld.com/the-company/blog/articles/alfa-romeo-pandion/

[8] Bertone Alfa Romeo Pandion. Wikimedia [online]. [cit. 2017-05-18]. Retrieved from: https://upload.wikimedia.org/wikipedia/commons/1/12/Bertone_-_Alfa_Romeo_Pandion_(84).JPG

[9] Tata Pixel: International show in Geneva. Car Advice [online]. [cit. 2017-05-18]. Retrieved from: http://s3.caradvice.com.au/wp-content/uploads/2011/03/tata-pixel-concept-51.jpg

[10] Toyota Concept i. Aolcdn [online]. [cit. 2017-05-18]. Retrieved from: http://o.aolcdn.com/dims-global/dims3/GLOB/legacy_thumbnail/750x422/quality/95/https:/s.blogcdn.com/slideshows/images/slides/433/359/4/S4333594/slug/l/06-toyota-concept-i-1.jpg

[11] Waterfall model. Exam Certification [online]. [cit. 2017-05-18]. Retrieved from: http://istqbexamcertification.com/what-is-waterfall-model-advantages-disadvantages-and-when-to-use-it/

[12] FRAZÉN, Anton, Sebastian KATRA a Lewis HORNE. Uniti - Ingenious Eletric Car: Technical Overview [online]. Sweden, 2016 [cit. 2016-10-30]

[13] Material properties. Web.mit.edu [online]. 2016 [cit. 2016-11-03]. Retrieved from: http://web.mit.edu/course/3/3.11/www/modules/props.pdf

[14] Automotive Safety Integrity Level. Wikipedia.org [online]. [cit. 2017-05-18]. Retrieved from: https://en.wikipedia.org/wiki/Automotive_Safety_Integrity_Level

[15] Torsional spring calculation. Mechanical, Industrial and Technical Calculations [online]. [cit. 2017-05-18]. Retrieved from: http://www.mitcalc.com/doc/sprtorsion/help/pic/SpringTorsion2.gif

[16] CNC kit. Media Cache [online]. [cit. 2017-05-19]. Retrieved from: https://s-media-cache-ak0.pinimg.com/236x/02/09/96/020996de5574c8dc9432b6dd70353427.jpg

[17] Hydraulic actuator description. Digital Connect Magazine [online]. [cit. 2017-05-19]. Retrieved from: http://www.digitalconnectmag.com/wp-content/uploads/2016/08/linear-actuator_650x387.jpg

[18] Plastic pinions. QTC Metric gears [online]. [cit. 2017-05-19]. Retrieved from: http://qtcgears.com/products/prodimgs/pinions/KFRCP.jpg

[19] Gas Springs. Wikipedia.org [online]. [cit. 2017-05-19]. Retrieved from: https://en.wikipedia.org/wiki/Gas_spring

[20] Gas Struts. Alibaba [online]. [cit. 2017-05-19]. Retrieved from: https://guideimg.alibaba.com/images/shop/78/09/18/0/ford-focus-estate-1998-2001-tailgate-lifter-gas-struts-with-oem-fittings-in-black-carbon-steel-with-nitrocarburized-plating_5090030.jpg

[21] Mechanism dynamic option: Simulation software. PTC [online]. [cit. 2017-05-19]. Retrieved from: http://www.ptc.com/cad/creo/parametric/mechanism-dynamics-option

[22] Beaufort scale: Weather Conditions. Wikipedia.org [online]. [cit. 2017-05-21]. Retrieved from: https://en.wikipedia.org/wiki/Beaufort_scale

[23] Center of Pressure. National aeronautics and space administration: NASA [online]. 2015 [cit. 2017-05-21]. Retrieved from: https://www.grc.nasa.gov/www/k-12/airplane/cp.html

[24] LinMot: Short motor types [online]. [cit. 2017-05-21]. Retrieved from: http://shop.linmot.com/E/flexsearchresults/linear-motors/linear-motors-p01-37/stators-ps01-37x120-hp/ps01-37sx120f-hp-n-agi.htm

[25] Teknic: Brushless servomotors [online]. [cit. 2017-05-21]. Retrieved from: https://www.teknic.com/compare-models/

[26] Spur Gear: Parameters [online]. [cit. 2017-05-21]. Retrieved from: https://static1.squarespace.com/static/5162dd74e4b0715db6231597/t/5174fe9ee4b010aac956fa6f/1434564379497/model3.png

[27] ING. JAN KOLOUCH. Strojní součásti z plastů. Praha: SNTL - Nakladatelství technické literatury, 1981. 260 s. ISBN 04-234-81.

[28] MM PRŮMYSLOVÉ SPEKTRUM. Ozubená kola [online]. Vydání 4/2006, URL:< http://www.mmspektrum.com/pdf/c060412.pdf

[29] Engineering plastics: Licharz engineering plastics. Tecno Plastics: Licharz engineering plastics [online]. 2004 [cit. 2017-05-21].

[30] Polyetheretherketone: Datasheet. Bearing works [online]. [cit. 2017-05-22]. Retrieved from: https://www.bearingworks.com/uploaded-assets/pdfs/retainers/peek-datasheet.pdf

[31] Hepco Linear Ball Guides: Datasheet. Hepco web [online]. [cit. 2017-05-22]. Retrieved from: https://hepcomotion.partcommunity.com/3d-cad-models/FileService/File/hepcomotion/34_hlg/mlg_series/hlg_01_uk_jan_16.pdf/

[32] Curvi Line: Brochures. ROLLCO [online]. [cit. 2017-05-22]. Retrieved from: http://www.rollco.se/fileadmin/user_upload/Rollco/Brochures/Curvi_Line.pdf

[33] Tesla Falcon door. Car and Driver: Blog [online]. [cit. 2017-05-27]. Retrieved from: http://blog.caranddriver.com/musk-attributes-falcon-wing-door-debacle-to-hubris-says-software-will-fix-it/

[34] Tesla may have disabled the Model X's door safety sensors. Engadget: Transportation [online]. 2016 [cit. 2017-05-27]. Retrieved from: https://www.engadget.com/2016/09/02/tesla-model-x-falcon-wing-door-sensor/

[35] Electrical safety edges. Bricher reglomat [online]. 2017 [cit. 2017-05-27]. Retrieved from: http://reglomat.bircher.com/en_us/detectors-and-switches-from-bircher-reglomat-delivered-worldwide/electrical-safety-edges-for-automatic-door-and-gate-systems/

[36] Sensing Edges for Automated Gates. Miller Edge: Making your world a safer place [online]. 2017 [cit. 2017-05-27]. Retrieved from: http://www.milleredge.com/how-miller-edge-works.html

[37] Touch Sensors. Electronics hub: Making your world a safer place [online]. 2015 [cit. 2017-05-27]. Retrieved from: http://www.electronicshub.org/touch-sensors/

LIST OF SYMBOLS

M	[-]	mobility of system
a_1	[mms^{-2}]	instantaneous acceleration of door cog
a_d	[mm]	distance between pinion axis and curved gear axis
b_{1F}	[mm]	pinion face width
b_2	[mm]	nominal key width
b_{2F}	[mm]	curved gear rack width
b_{MAX}	[mm]	maximal face width
C_1	[-]	correlational coefficient
C_2	[-]	correlational coefficient
c_3	[mm]	distance between door centre of gravity and rail (in z-axis direction)
c_{a1}	[mm]	pinion gear clearance
c_{a2}	[mm]	curved gear rack clearance
d_1	[m]	distance between door cog and axis of front axle
D_1	[mm]	pitch circle diameter of drive gear
d_2	[m]	distance between centre of pressure and door attachment point
D_2	[mm]	pitch circle diameter of driven gear
D_3	[mm]	diameter of motor output shaft
d_3	[mm]	distance between centre of pressure and rail (in y-axis direction)
d_4	[mm]	distance between door centre of gravity and rail (in x-axis direction)
d_5	[mm]	distance between door centre of gravity and rail (in z-axis direction)
d_6	[mm]	distance between D_2 and door cog trajectory
d_7	[mm]	distance between rotary actuator and axis of axis of hole
d_8	[mm]	distance between centre of actuator housing and force reaction F_R
D_{a1}	[mm]	pinion addendum circle diameter
D_{a1MAX}	[mm]	maximal addendum circle diameter for pinion
D_{a1MAX}	[mm]	maximal addendum circle diameter for curved rack
D_{a2}	[mm]	curved gear rack addendum circle diameter
D_b	[mm]	bolt size
D_{f1}	[mm]	pinion base circle diameter
D_{f2}	[mm]	pinion base circle diameter
D_p	[mm]	pitch diameter
E_{PEEK}	[GPa]	modulus of elasticity of modified polyetherketone

f_1	[-]	friction diameter between door and curved gear rail
F_1	[N]	force of linear actuator
F_3	[N]	force of shaft on key
F_A	[N]	aerodynamic force
F_b	[N]	operational force from moment acting on one screw
F_G	[N]	gravitational force
F_{GA}	[N]	axial component of gravitational force
F_{GR}	[N]	radial component of gravitational force
f_i	[-]	degree of freedom
F_R	[N]	radial force
F_{R1}	[N]	radial force 1
F_{R2}	[N]	radial force 2
F_{R3}	[N]	radial force 3
F_{R4}	[N]	radial force 4
F_{SC}	[N]	centripetal force
F_{TX}	[N]	force acting at point T in x-axis
F_{TY}	[N]	force acting at point T in y-axis
F_U	[N]	maximal peripheral force
g	[ms^{-2}]	gravitational acceleration
h	[m]	elevation of point above a reference plane
h_1	[mm]	pinon teeth high
h_2	[mm]	curved gear rack high
$i_{1,2}$	[-]	gear ratio between rotary actuator and door
I_z	[kgm^2]	moment of inertia in door cog parallel to rotational axis
k_1	[-]	safety factor related to the tooth root stress analysis
k_2	[-]	safety factor related to the key shear stress analysis
k_3	[-]	safety factor related to bearing stress analysis
k_4	[-]	safety factor related to elasticity limit of bolt yield stress
K_B	[-]	operating factor for different types of drive operation
l_1	[mm]	nominal key length
m	[-]	modul
m_1	[kg]	door weight
M_1	[Nm]	moment of rotary actuator

M_2	[Nm]	applied moment on output shaft
M_T	[Nm]	moment
M_x	[Nm]	moment developed by aerodynamic force
M_{XLIN}	[Nm]	moment applied on linear rail in x-axis
M_{YLIN1}	[Nm]	moment applied on linear rail in y-axis developed by force F_1
M_{YLIN2}	[Nm]	moment applied on linear rail in y-axis developed by force F_U
M_{ZLIN}	[Nm]	moment applied on linear rail in z-axis
n_{1max}	[min^{-1}]	maximum speed of drive gear
n_{2max}	[min^{-1}]	maximum door speed
n_b	[-]	number of used bolts
n_J	[-]	number of joints
n_L	[-]	number of links
n_t	[-]	number of screwed threds inside each insert
p	[Pa]	fluid pressure
p_1	[MPa]	bearing stress
P_1	[W]	performance of linear actuator
P_{1P}	[mm]	pinion circular pitch
P_2	[W]	force of rotary actuator
P_{2P}	[mm]	curved gear rack circular pitch
p_p	[MPa]	permissible compressive stress of modified polyetherketone
p_t	[MPa]	pressure in threads
R_{el}	[MPa]	bolt yield strength
S_1	[m^2]	projected area (right side) of door in open position
S_2	[m^2]	projected area (left side) of door in open position
s_1	[mm]	trajectory distance of door cog
t_1	[mm]	nominal keyway depth in shaft
t_2	[mm]	nominal keyway depth in pinion
v_1	[mms^{-1}]	instantaneous velocity of door cog
v_2	[ms^{-1}]	fluid flow velocity
W_1	[J]	energy of linear actuator
w_1	[mm]	pinion width of space
W_2	[J]	performance of rotary actuator
w_2	[mm]	curved gear rack width space

Y_F	[-]	tooth shape factor
Y_β	[-]	helix factor
z_1	[-]	number of teeth on input gear
z_2	[-]	number of teeth on output gear
α_1	[deg]	angle of door in closed position relatively to ground
α_1	[$degs^{-2}$]	instantaneous angular acceleration of door cog
α_2	[deg]	angle of door in opened position relatively to ground
δ	[mm]	maximal displacement of actuator housing
μ_1	[-]	coefficient
μ_2	[-]	coefficient
ρ	[kgm^{-3}]	fluid density
P_{PEEK}	[kgm^3]	density of modified polyetherketone
σ_1	[-]	coefficient
σ_2	[-]	coefficient
σ_F	[MPa]	tooth root stress
σ_{PEEK}	[MPa]	yield stress of modified polyetherketone
σ_{RED}	[MPa]	maximal von Mises stress value
τ_d	[MPa]	permissible shear stress of modified polyetherketone
τ_S	[MPa]	shear stress developed by force of shaft on key
ϕ_1	[deg]	angle
ω_1	[$degs^{-1}$]	instantaneous angular velocity of door cog
ω_{1MAX}	[$rads^{-1}$]	maximal instantaneous angular velocity of door cog

LIST OF FIGURES

LIST OF TABLES

APPENDIX

Kinematic characteristics of linear door motion (distance, translation speed, acceleration)

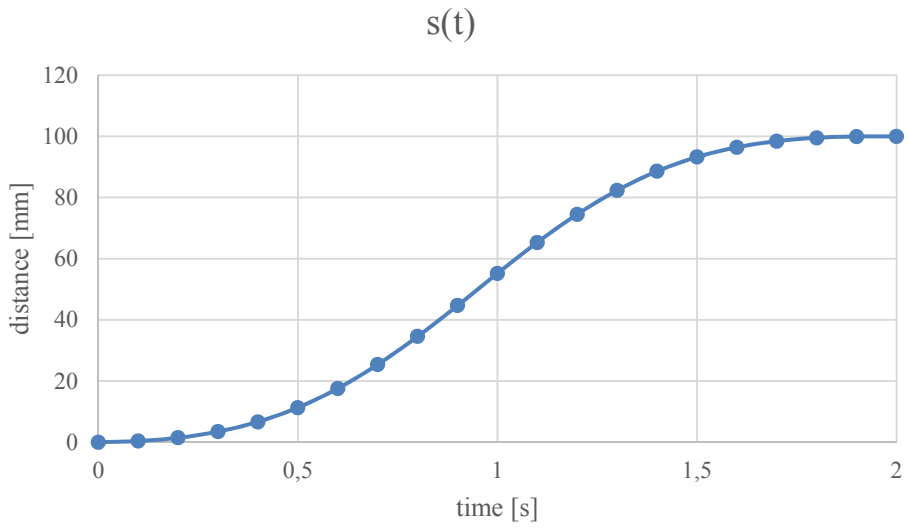

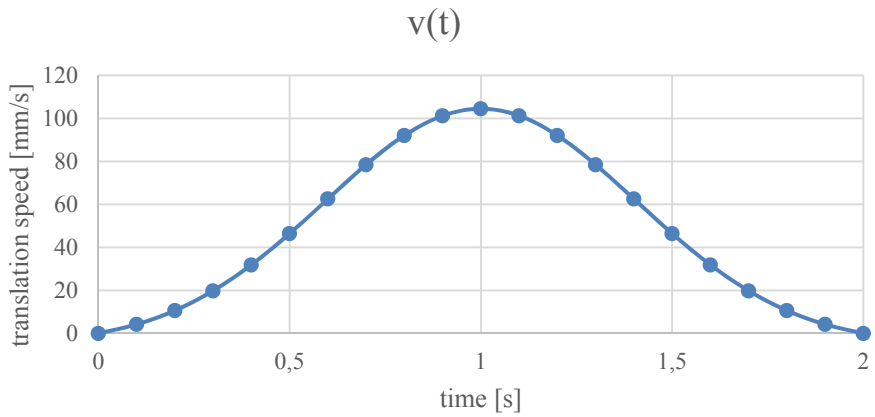

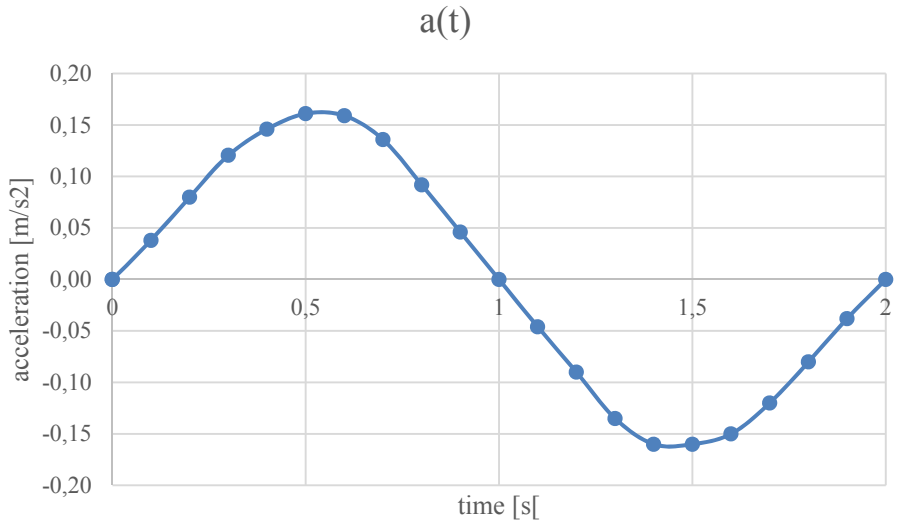

Kinematic characteristics of rotational door motion (angular position, angular speed, angular acceleration)

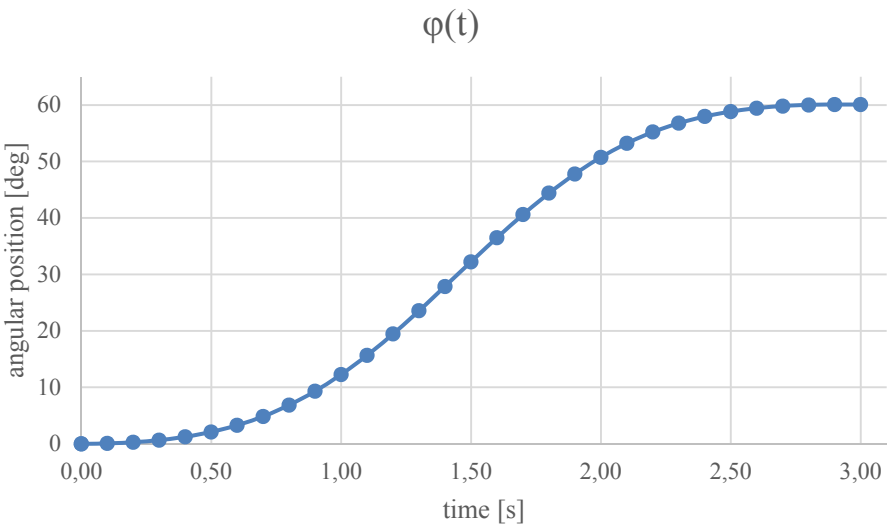

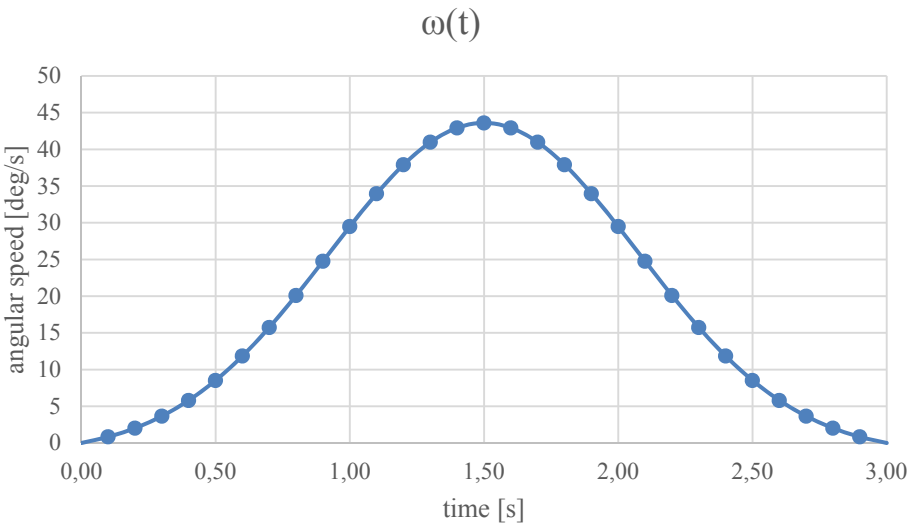

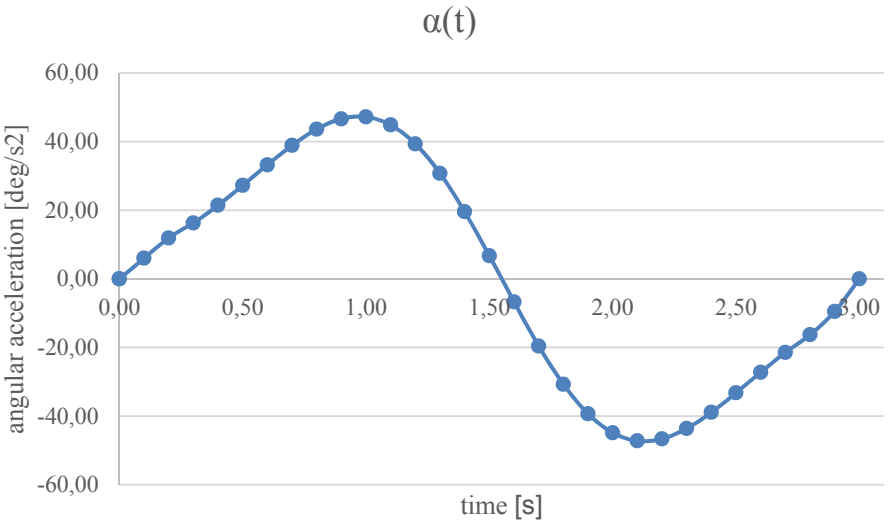

Bolt calculation

Výpočet počtu šroubů pro přenos momentu mezi ozubením a dveřmi

Maximální přenášený moment: $Mk := 148.3N \cdot m$

Průměr šroubu M5: $d := 5mm$

Roztečná kružnice šroubů: $D := 736mm$

Počet šroubů: $i := 4$

Návrhový součinitel: $kn := 2$

Součinitel tření mezi ozubením a dveřmi: $fs := 0.4$

Součinitel tření v závitech: $f := 0.2$

Součinitel tření pod hlavou šroubu: $fo := 0.4$

Provozní síla od momentu působící na 1 šroub kolmo k jeho ose: $F := \frac{2Mk}{D \cdot i} = 100.747N$

Potřebná síla předpětí 1 šroubu: $Fi := \frac{kn \cdot F}{fs} = 503.736N$

Kontrola šroubu:

Stoupání závitu: $P := 1mm$

Úhel profilu metrického závitu ISO: $\alpha := 60deg$

Výpočtový průřez šroubu: $As := 28.27mm^2$

Výška základního trojúhelníku: $H := 0.5 \cdot \sqrt{3} \cdot P = 0.866 \cdot mm$

Střední průměr závitu šroubu: $d2 := d - \frac{3 \cdot H}{4} = 4.35 \cdot mm$

Malý průměr ve vrcholu zaoblení závitového dna: $d3 := d - \frac{17 \cdot H}{12} = 3.773 \cdot mm$

Stoupání jednochodého závitu P=Ph: $Ph := 1mm$

Napětí od síly předpětí: $\sigma := \frac{Fi}{As} = 17.819 \cdot MPa$

Smykové napětí ve šroubu: $\tau := \frac{16 \cdot \left[\frac{Fi \cdot d2}{2} \cdot \left(\frac{Ph + \pi \cdot f \cdot d2 \cdot \sec(\alpha \cdot 0.5)}{\pi \cdot d2 - f \cdot Ph \cdot \sec(\alpha \cdot 0.5)} \right) \right]}{\pi \cdot d3^3} = 32.137 \cdot MPa$

Redukované napětí dle HMH: $\sigma red := \sqrt{\sigma^2 + 3 \cdot \tau^2} = 58.445 \cdot MPa$

Mez kluzu šroubů třídy 6.6 $R\_e := 480MPa$

Bezpečnost vůči MSP: $kk := \frac{R\_e}{\sigma red} = 8.213$

Kontrola tlaku v závitech:

Výpočet malého průměru závitu matice: $D1 := d - \frac{10 \cdot H}{8} = 3.917 \cdot mm$

Délka zašroubování šroubu v matici: $l\_unaš := 10mm$

Počet zašroubovaných závitů v matici: $nz := \frac{l\_unaš}{P} = 10$

Tlak v závitech za předpokladu rovnoměrného rozložení: $p := \frac{Fi}{nz \cdot \frac{\pi \cdot \left(d^2 - D1^2\right)}{4}} = 6.644 \cdot MPa$

Navrhovaný spoj vyhovuje pevnostním požadavkům

			HAZARD IDENTIFICATION			CLASSIFICATION OF HAZARDOUS EVENTS									
Nr.	Component		Possible malfunction	Situation		S	Argument		E	Argument		C	Argument		ASIL		Safety Goal
1	Actuator	1.1	door injures a passanger during the closing process	Passenger is injured by the door during the closing process, door mechanism is not able to reduce force or stop when some obstacle occurs.		3	Without the possibility to slow down closing speed participants could be badly injured or killed.		4	Regular entrance inside the vehicle.		3	Passengers can be injured due to high closing speed and no possibility to stop door movement.		D		Active regulation of speed with possibility to stop door movement.
		1.2	door will open without passanger´s command	Fully occupied vehicle; higher speed; passengers do not use seat belts.		3	Passangers can leave the car and hurt themselfs during the drive.		4	Regular driving situation.		3	Passengers can die if they will not use seat belts and they will exit the vehicle in high or medium speed.		D		Mechanical door movement prevention will activate when the vehicle speed will extend 5kph.
				Fully occupied vehicle; higher speed during vehicle cornering effects high lateral acceleration; passengers do not use seat belts		3	Passengers can exit the car and hurt themselves during the drive.		4	High or medium speed cornering.		3	Passengers can die if they will not use seat belts and they will exit the vehicle in high or medium speed.		D		Mechanical door movement prevention will activate when the vehicle speed will extend 5kph.
		1.4	passanger can not open the door	System does not allow open the door when the passenger is inside the vehicle.		1	Without possibility to exit the car, passenger must demage the door structure.		4	Regular driving situation.		1	Passengers can remain in the vehicle.		QM		The door must be manually openable by passengers.
				System does not allow open the door when the passenger wants to get inside the car.		0	Car stays stationary.		4	Participants use the system everytime when they start the car.		0	Driving mode is not possible.		QM		Loss of electric contact (by fault), or mechanical failure must be avoided.

Hazard analysis

P01-37Sx120F/40x120-HP

LinMot®

Max. Stroke: 120mm
Max. Force: 255N

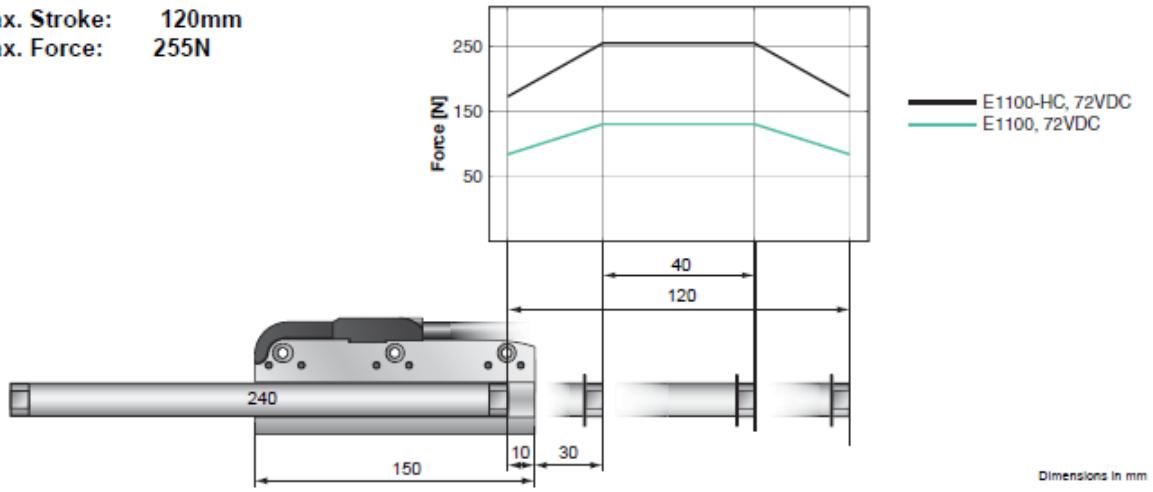

Motor Specification		
Stator		Standard Winding
Slider		High Performance High Performance Heavy Duty
Standard Stroke SS	mm (in)	40 (1.57)
Extended Stroke ES	mm (in)	120 (4.72)
Max. Force	N (lbf)	255 (57.3)
Cont. Force	N (lbf)	35 (7.87)
Cont. Force with fan	N (lbf)	65 (14.6)
Max. Velocity	m/s (in/s)	3.9 (154)
Max. Current	A_{pk}	15
Cont. Current	A_{pk}	2.35
Cont. Current with fan	A_{pk}	4.10
Force Constant	N/A (lbf/A)	17 (3.83)
Border Force	%	67
Linearity	%	±0.1
Slider Length	mm (in)	240 (8.45)
Slider Mass	g (lb)	510 (1.12)

Characteristic of linear actuator